

University of Kentucky

UKnowledge

---

Microbiology, Immunology, and Molecular  
Genetics Faculty Publications

Microbiology, Immunology, and Molecular  
Genetics

---

6-1-2017

## Zinc Transporters YbtX and ZnuABC Are Required for the Virulence of *Yersinia pestis* in Bubonic and Pneumonic Plague in Mice


Alexander G. Bobrov  
*Washington State University*

Olga Kirillina  
*Washington State University*

Marina Y. Fosso  
*University of Kentucky*, marina.fosso@uky.edu

Jacqueline D. Fetherston  
*University of Kentucky*, jdfeth01@uky.edu

M. Clarke Miller additional works at: [https://uknowledge.uky.edu/microbio\\_facpub](https://uknowledge.uky.edu/microbio_facpub)

 *University of North Georgia*  
Part of the [Bacteria Commons](#), [Medical Immunology Commons](#), [Medical Microbiology Commons](#),  
[Molecular Genetics Commons](#), and the [Pathology Commons](#)

[Click here to provide feedback](#) in a new tab to let us know how this document benefits you.

---

### Repository Citation

Bobrov, Alexander G.; Kirillina, Olga; Fosso, Marina Y.; Fetherston, Jacqueline D.; Miller, M. Clarke; VanCleave, Tiva T.; Burlison, Joseph A.; Arnold, William K.; Lawrenz, Matthew B.; Garneau-Tsodikova, Sylvie; and Perry, Robert D., "Zinc Transporters YbtX and ZnuABC Are Required for the Virulence of *Yersinia pestis* in Bubonic and Pneumonic Plague in Mice" (2017). *Microbiology, Immunology, and Molecular Genetics Faculty Publications*. 139.  
[https://uknowledge.uky.edu/microbio\\_facpub/139](https://uknowledge.uky.edu/microbio_facpub/139)

This Article is brought to you for free and open access by the Microbiology, Immunology, and Molecular Genetics at UKnowledge. It has been accepted for inclusion in Microbiology, Immunology, and Molecular Genetics Faculty Publications by an authorized administrator of UKnowledge. For more information, please contact [UKnowledge@lsv.uky.edu](mailto:UKnowledge@lsv.uky.edu).

---

## Zinc Transporters YbtX and ZnuABC Are Required for the Virulence of *Yersinia pestis* in Bubonic and Pneumonic Plague in Mice

Digital Object Identifier (DOI)

<https://doi.org/10.1039/C7MT00126F>

### Notes/Citation Information

Published in *Metallomics*, v. 9, issue 6, p. 757-772.

This journal is © The Royal Society of Chemistry 2017

The copyright holder has granted the permission for posting the article here.

The document available for download is the authors' post-peer-review final draft of the article.

### Authors

Alexander G. Bobrov, Olga Kirillina, Marina Y. Fosso, Jacqueline D. Fetherston, M. Clarke Miller, Tiva T. VanCleave, Joseph A. Burlison, William K. Arnold, Matthew B. Lawrenz, Sylvie Garneau-Tsodikova, and Robert D. Perry



# HHS Public Access

Author manuscript

*Metallomics*. Author manuscript; available in PMC 2018 June 21.

Published in final edited form as:

*Metallomics*. 2017 June 21; 9(6): 757–772. doi:10.1039/c7mt00126f.

## Zinc transporters YbtX and ZnuABC are required for the virulence of *Yersinia pestis* in bubonic and pneumonic plague in mice

Alexander G. Bobrov<sup>a,\*</sup>, Olga Kirillina<sup>a,\*</sup>, Marina Y. Fosso<sup>b</sup>, Jacqueline D. Fetherston<sup>a</sup>, M. Clarke Miller<sup>c</sup>, Tiva T. VanCleave<sup>d</sup>, Joseph A. Burlison<sup>e</sup>, William K. Arnold<sup>a</sup>, Matthew B. Lawrenz<sup>d</sup>, Sylvie Garneau-Tsodikova<sup>b</sup>, and Robert D. Perry<sup>a,‡</sup>

<sup>a</sup>Department of Microbiology, Immunology, and Molecular Genetics, University of Kentucky, Lexington, KY, USA

<sup>b</sup>Department of Pharmaceutical Sciences, University of Kentucky, Lexington, KY, USA

<sup>c</sup>Department of Chemistry and Biochemistry, University of North Georgia, Gainesville, GA, USA

<sup>d</sup>Department of Microbiology and Immunology, Center for Predictive Medicine, University of Louisville School of Medicine, Louisville, KY, USA

<sup>e</sup>James Graham Brown Cancer Center, University of Louisville, Louisville, KY, USA

### Abstract

A number of bacterial pathogens require the ZnuABC Zinc ( $Zn^{2+}$ ) transporter and/or a second  $Zn^{2+}$  transport system to overcome  $Zn^{2+}$  sequestration by mammalian hosts. Previously we have shown that in addition to ZnuABC, *Yersinia pestis* possesses a second  $Zn^{2+}$  transporter that involves components of the yersiniabactin (Ybt), siderophore-dependent iron transport system. Synthesis of the Ybt siderophore and YbtX, a member of the major facilitator superfamily, are both critical components of the second  $Zn^{2+}$  transport system.

Here we demonstrate that a *ybtX znu* double mutant is essentially avirulent in mouse models of bubonic and pneumonic plague while a *ybtX* mutant retains high virulence in both plague models. While sequestration of host Zn is a key nutritional immunity factor, excess Zn appears to have a significant antimicrobial role in controlling intracellular bacterial survival. Here, we demonstrate that ZntA, a  $Zn^{2+}$  exporter, plays a role in resistance to Zn toxicity *in vitro*, but that a *zntA zur* double mutant retains high virulence in both pneumonic and bubonic plague models and survival in macrophages. We also confirm that Ybt does not directly bind  $Zn^{2+}$  *in vitro* under the conditions tested. However, we detect a significant increase in  $Zn^{2+}$ -binding ability of filtered supernatants from a Ybt<sup>+</sup> strain compared to those from a strain unable to produce the siderophore, supporting our previously published data that Ybt biosynthetic genes are involved in the production of a secreted Zn-binding molecule (zincophore). Our data suggest that Ybt or a modified Ybt participate in or promote Zn-binding activity in culture supernatants and is involved in Zn acquisition in *Y. pestis*.

<sup>‡</sup>For correspondence. rperry@uky.edu; Tel (+1) 859 323-6341; Fax (+1) 859 257 8994.

<sup>\*</sup>A.G. Bobrov and O. Kirillina contributed equally to this study and are co-first authors; The current address for both is Department of Veterinary Microbiology, Paul G. Allen School of Global Animal Health, Washington State University, Pullman, WA, USA

## Introduction

Zinc (Zn) is an essential transition metal for archaeal, bacterial, and eukaryotic organisms where it serves both catalytic and structural functions.<sup>1-4</sup> In recent years, the definition of metal nutritional immunity has been expanded to include zinc ions, Zn<sup>2+</sup>, (and manganese [Mn<sup>2+</sup>] as well as other biometals and organic compounds) as mammalian hosts attempt to restrict the availability of Zn<sup>2+</sup> to invading pathogens. Serum Zn levels are chelated by a variety of proteins and this metal is further sequestered, both locally and systemically upon infection.<sup>5-16</sup>

Consequently, like iron (Fe), bacterial high affinity Zn<sup>2+</sup> uptake systems are important for the virulence of a number of bacterial pathogens.<sup>17-40</sup> However, only a relatively small number of different uptake mechanisms have been identified in these pathogens. The ZnuABC family of ABC transporters is the most common with a second periplasmic Zn<sup>2+</sup>-binding protein, ZinT, working through the Znu system in some bacteria in conjunction with ZnuA, the primary periplasmic Zn<sup>2+</sup>-binding protein of the ZnuABC system.<sup>2, 41-43</sup> Although described as a low-affinity Zn<sup>2+</sup> transporter, ZupT, a ZIP family proton motive force-dependent transporter, functions at micromolar Zn<sup>2+</sup> levels *in vitro*, and plays a role in the virulence of *Escherichia coli* UPEC and *Salmonella*.<sup>21, 28, 38, 44</sup> Two additional inner membrane (IM) transporters (ZevAb and ZurAM) have been identified in *Haemophilus influenzae* and *Listeria monocytogenes*, respectively.<sup>22, 37</sup>

Recently, we demonstrated that HMWP2 (encoded by *irp2*), a nonribosomal peptide synthetase required for synthesis of the yersiniabactin (Ybt) siderophore, and the putative IM protein YbtX are both involved in Zn<sup>2+</sup> uptake in *Yersinia pestis*, the causative agent of bubonic, septicemic, and pneumonic plague.<sup>45</sup> *In vitro*, single *irp2::kan* and *irp2* mutants (KIM6-2046.1 and KIM6-2046.3, respectively) have no growth defect in the Chelex-100 treated defined medium PMH2 (cPMH2; residual Fe and Zn<sup>2+</sup> concentrations of ~0.3 and ~0.5 μM, respectively) while a single *znuBC* mutant (KIM6-2077+) has a significant growth defect in this medium. The *irp2::kan znuBC* double mutant (KIM6-2077.7) is unable to grow in cPMH2 unless supplemented with Zn<sup>2+</sup> at 2.5 μM. Intriguingly, YbtX, a member of the Major Facilitator Superfamily (MFS), but not Psn, TonB, or YbtPQ (required for Fe<sup>3+</sup> uptake *via* Ybt) is required for Ybt-dependent acquisition of Zn<sup>2+</sup>. Finally, single *irp2::kan* and *znuBC* mutants retain high virulence in a mouse model of septicemic plague while the *irp2::kan znuBC* double mutant shows a > 4.3 × 10<sup>5</sup>-fold virulence loss in this model.<sup>45</sup>

While secreted Zn<sup>2+</sup>-chelating compounds (zincophores) have been proposed as a Zn<sup>2+</sup>-acquisition mechanism for pathogens,<sup>8</sup> examples of Zn<sup>2+</sup>-binding by secreted compounds and subsequent delivery to the bacterial cell for nutritional use are limited. The 33-kDa secreted Pra1 protein of the fungal pathogen *Candida albicans* binds Zn<sup>2+</sup> and a *pra1* mutant has reduced hyphal growth on endothelial cells that is alleviated by Zn<sup>2+</sup> supplementation.<sup>46</sup> The plant pathogen *Pseudomonas putida* produces a small siderophore, pyridine-2,6-bis(thiocarboxylic acid) (PDTC) that binds Fe<sup>3+</sup> and Zn<sup>2+</sup> and delivers these cations to the bacterial cell.<sup>47, 48</sup> *Streptomyces coelicolor* produces a siderophore-like

molecule, coelibactin, which has been proposed, but not proven, as a zincophore.<sup>49, 50</sup> In addition, the *Pseudomonas aeruginosa* siderophores pyochelin and pyoverdine bind a variety of cations, including  $Zn^{2+}$ , but nutritional delivery to the bacterial cell has not been tested. Instead, it has been proposed that this metal chelation may promote resistance to metal toxicity.<sup>51-53</sup> Finally, *Pseudomonas* spp and *Ralstonia solanacearum* produce micacocidin, a compound with a chemical structure similar to Ybt, which has been crystallized with  $Zn^{2+}$ ,  $Mn^{2+}$ , and  $Fe^{3+}$ .<sup>54, 55</sup>

Here we show the importance of ZnuABC and YbtX in  $Zn^{2+}$  acquisition in mouse models of bubonic and pneumonic plague and investigate the mechanism of Ybt-dependent  $Zn^{2+}$  uptake in *Y. pestis*. Finally, while Zn toxicity plays a role in controlling intracellular bacterial survival, we show that a *zntA zur::kan* mutant retains high virulence in mouse models of bubonic and pneumonic plague as well as survival in macrophages. In contrast, ZntA plays an important role in resistance to Zn toxicity *in vitro*.

## Experimental

### Bacterial strains, plasmids, primers and growth conditions

The bacterial strains, plasmids and primers used in this study are listed in Table S1 in supplemental material. *E. coli* strains DH5 $\alpha$  and DH5 $\alpha$  ( $\lambda$ pir) were used in construction and maintenance of recombinant plasmids and were grown in Luria broth (LB) or on LB agar at 28-37°C. For *Y. pestis* KIM strains, a plus sign indicates an intact chromosomal 102-kb *pgm* locus. All other *Y. pestis* strains have a mutation within this locus or a deletion of the entire locus. Genes which encode for the synthesis and transport of Ybt as well as transcriptional regulation of *ybt* genes are encoded within the *pgm* locus. *Y. pestis* avirulent strains lacking the pCD1 virulence plasmid were used for construction of mutants and for *in vitro* studies. The *Y. pestis* strains were grown in autoclaved Heart Infusion Broth (HIB), Brain Heart Infusion (BHI) or on Tryptose Blood Agar Base (TBA) (Difco) at 26-33°C. For some experiments, HIB that was sterilized by passage through 0.22  $\mu$ m filters (Millipore) (HIB-FS) was used. Where necessary, ampicillin (Ap), chloramphenicol (Cm), kanamycin (Km), streptomycin (Sm), or tetracycline (Tc) were routinely used at final concentrations of 100, 30 or 15, 50, 50, and 12.5  $\mu$ g ml<sup>-1</sup>, respectively, unless noted otherwise.

For metal-deficient growth studies glassware was cleaned with a chromic-sulfuric acid solution to remove contaminating metals as previously described.<sup>56</sup> Metal-deficient, chemically defined media PMH or PMH2 (cPMH or cPMH2, respectively) were prepared as described previously using Chelex-100.<sup>56-58</sup> *Y. pestis* strains were inoculated from -80°C glycerol stocks onto TBA supplemented with 0.2% galactose, Congo red (TBA-CR) and  $ZnSO_4$  or  $ZnCl_2$  at final concentrations of 100  $\mu$ g ml<sup>-1</sup> and 10  $\mu$ M, respectively and grown at 32-33°C for 2 days. Cells which bind CR have retained the *pgm* locus. CR positive cells (red colonies) were grown on TBA slants at 32-33°C overnight and then inoculated to an OD<sub>620</sub> of ~0.1 in cPMH2 with  $ZnCl_2$  and  $FeCl_3$  added to final concentrations of 0.6  $\mu$ M and 1  $\mu$ M where indicated, respectively. Growth of the cultures was monitored by determining the OD<sub>620</sub> with a Genesys5 spectrophotometer (Spectronic Instruments, Inc.).

For Zn toxicity assays, *Y. pestis* cultures grown in HIB-FS medium were back diluted to an OD<sub>620</sub> of ~0.025 in HIB-FS containing a range of ZnSO<sub>4</sub> concentrations from 0 to 800 μM. Cultures were grown overnight and the final OD<sub>620</sub> was measured. In all assays, bacteria were grown at 37°C with shaking.

### Mutant strain construction

Suicide plasmids pSucZnu3.5, pKNG *znuA*, and pZur4 were used to introduce mutations *znuBC*, *znuA*, and *zur::kan* respectively, into various *Y. pestis* KIM strains by allelic exchange and confirmed by PCR as described previously.<sup>45, 59</sup> TBA medium supplemented with 5% sucrose (TBAS) was used to excise integrated suicide vectors expressing SacB. Plasmid isolation and sensitivity to the appropriate antibiotic was used to confirm loss of the suicide vectors. All bacterial strains, plasmids and primers used in this study are listed in Table S1 in supplemental material.

To replace *zntA* with a *cam* cassette, Y0410red-1 and Y0410red-2 primers were used to prepare a PCR product from pKD3 which was transformed into KIM6(pWL204)+; the *zntA::cam2196* mutation was verified with primers Y0410-pBAD-F and Cm-2 (Table S1). The *cam* cassette was removed using pSkippy<sup>60</sup> and confirmed by demonstrating that the resulting strain was now Cm sensitive. Growth on TBAS plates was used to cure strains of pWL204 and pSkippy and their loss was confirmed by plasmid analysis and restoration of antibiotic sensitivities. Using suicide vector pZur4, *zur*<sup>+</sup> was inactivated in the *zntA* mutant (KIM6-2196.1+). The presence of the *zur::kan2078* mutation in the resulting *zntA zur::kan* strain, designated KIM6-2196.4+, was verified by PCR using primers zur3.3 and zur5.3 as described previously.<sup>59</sup>

The gene *y3657* was replaced with a *kan* cassette from pKD4 in KIM6-2077+ (*znuBC*). The PCR product was prepared using Y3657red-F and Y3657Rred-R, transformed into KIM6-2077(pWL204)+ and Km<sup>r</sup> colonies were streaked onto TBAS plates to eliminate pWL204. The *y3657::kan2203* mutation was verified by PCR using primers KM-1 and Y3657 del. One confirmed mutant was named KIM6-2202.1+ (*y3657::kan znuBC*) and used in subsequent experiments.

### Repair of the *ybtX* mutation

An ~ 2.64 kb fragment from the *ybtX* region of *Y. pestis* KIM10+ genomic DNA was amplified with Phusion HF polymerase (New England Biolabs) using primers YbtX-comp-*HindIII* and YbtX-comp-Rev. After purification and digestion with *HindIII*, the PCR product was cloned into the *HindIII* and *SmaI* sites of pWSK29 to generate pWSK-YbtX-comp. After the presence of the correct insert was confirmed by sequencing (ACGT) using primers pPQX-vector-2100 and pPQX-vector-1300, the plasmid was digested with *ApaI* and *BamHI* and a 2.67 fragment containing *ybtX*<sup>+</sup> was ligated into the *ApaI* and *BamHI* sites of pKNG101 generating pKNG-YbtX-comp. This suicide vector was electroporated into the *ybtX znuA* mutant (KIM6-2197.2). Incubation on TBAS plates selected for a strain in which the in-frame *ybtX2067* mutation was replaced by *ybtX*<sup>+</sup> resulting in the YbtX<sup>+</sup> Znu<sup>-</sup> strain KIM6-2197.4+ (*ybtX<sup>TP</sup> znuA*). The pWSK-YbtX-comp plasmid was also digested with *XhoI* and *BamHI* and a 2.66-fragment ligated into *SaII* and *BamHI* sites of pSR47s

generating pSR-YbtX-comp. In the BSL3 facility, this suicide plasmid was also used to restore *ybtX*<sup>+</sup> in KIM5-2197.2 (pCD1Ap), a *ybtX znuA* mutant carrying the virulence plasmid that encodes a type three secretion system, generating KIM5-2197.4(pCD1Ap)+ (*ybtX*<sup>TP</sup> *znuA*). The restoration of *ybtX*<sup>+</sup> in both strains was confirmed with primers P27 and P33.

### Cloning of *ybtX* expressed from the *znuA* promoter

Primers *ybtX*compl\_R6K\_R-SpeI and *ZnuA*prom-*ybtX*-BamHI (which includes 63 bp of the *znuA* promoter region and 23 bp containing a putative Shine-Dalgarno sequence upstream of the predicted translational start of *ybtX* ORF) were used to generate an ~ 1.6-kb fragment that contains the coding sequence for *ybtX* cloned downstream of the *znuA* promoter using Phusion HF polymerase (New England Biolabs) and the pYbtX plasmid<sup>45</sup> as a template. After purification, the PCR product was digested with *SpeI* and *BamHI* and ligated into the *XbaI* and *BamHI* sites of pACYC184 to generate pYbtX-ZP. The presence of the correct fragment was confirmed by sequencing (ACGT Inc.) and the plasmid was electroporated into KIM6-2097.1 ( *irp2 znuA*).

### Western Blot Analysis

Cells were grown at 37°C under metal-deficient conditions for two transfers, pelleted at 6000 × g for 10 minutes, resuspended in SDS-sample buffer at a final OD<sub>620</sub> of 10.0 and disrupted by vortexing with Zirconia beads. A 20 µl sample was loaded onto a 12.5% SDS gel and the proteins were electrophoresed at 80 V at room temperature. After electrophoresis, the gel was incubated in a carbonate transfer buffer (10 mM NaHCO<sub>3</sub>, 3mM Na<sub>2</sub>CO<sub>3</sub>, pH 9.9, 20% methanol) for 10 minutes on ice and the proteins transferred to a PVDF membrane at 100 mA in an ice bath overnight.<sup>61</sup> A 1:1000 dilution of antiserum to YbtX was used for detection. Rabbit antiserum against YbtX was made to a peptide (YIRLHSARELMYSAID) in the C-terminus of the protein (Open Biosystems, Inc.).

### Growth complementation with culture supernatants

Feeding assays with culture supernatants were performed as previously described.<sup>45</sup> Briefly, for supernatant preparation, cells were grown under metal-deficient conditions for two transfers (~6-8 generations), the cells pelleted and supernatants filter sterilized (0.22 µm Millipore). The *Y. pestis* recipient strain *irp2::kan psn znuBC* (KIM6-2077.18) was grown at 37°C in cPMH2 supplemented to 0.6 µM ZnCl<sub>2</sub> and 1 µM FeCl<sub>3</sub> for ~3-4 generations before diluting to an OD<sub>620</sub> of ~0.1 in the same medium containing 50% (v/v) culture supernatants from test strains. Bacteria were grown overnight and the final OD<sub>620</sub>s were measured.

### Apo-Ybt purification

Apo-Ybt was isolated and purified in a multi-step procedure slightly modified from previous methods.<sup>62, 63</sup> No iron was added to the spent medium before extraction. Eight liters of spent medium were extracted three times in 500 ml aliquots with 200 ml portions of ethyl acetate. The organic layers were combined and the solvent was removed by rotary evaporation at

40°C in the dark. The material was then dissolved in ~ 5 ml of absolute ethanol and then further diluted with 50 ml of 18 MΩ water for the next purification step.

The crude Ybt extract was dissolved in a 10:1 water-ethanol solution, loaded onto a 2.5 g pre-packed C<sub>18</sub> reverse phase cartridge, and purified on a 4.3 g C<sub>18</sub> reverse phase column with water and acetonitrile as the mobile phase using a Combiflash R<sub>f</sub>. The separation was achieved by using the following gradient: 10% acetonitrile for 3 min followed by a linear gradient from 10% to 70% acetonitrile over 25 min (R<sub>t</sub> for Yel ≈9 min and R<sub>t</sub> for Ybt ≈14 min for the Combiflash purification). Fractions were collected at 1 min intervals. During HPLC/MS analysis, two apo-Ybt peaks with retention times of 7.8 and 8.3 min were observed. In addition, two peaks with retention times of 5.6 and 5.9 min with the same *m/z* ratio of 297.07 were also observed; these truncated versions of Ybt are tentatively designated yersinol (Yel) and will be described in a separate study. Fractions containing apo-Ybt were combined and concentrated in the dark *via* rotary evaporation at 40°C. The purification protocol was repeated to afford apo-Ybt with excellent purity.

The identity and purity of compounds in each stage of purification were confirmed *via* mass spectrometry using an Agilent 6224 TOF LC/MS equipped with the Agilent 1260 HPLC system and MassHunter software. The instrument is equipped with an Agilent Extend C<sub>18</sub> column (1.8 μm, 2.1 × 50 mm) with mobile phase consisting of mass spectrometry grade water (with 0.1% formic acid and 0.1% methanol) and acetonitrile (with 0.1% formic acid) and operated in positive ion mode (3500 V Vcap, 750 V OctRF Vpp, 65 V skimmer, 135 V fragmenter, 40 psi Nebulizer gas, 12 L min<sup>-1</sup> drying gas, and 325°C gas temperature). Samples were eluted with a linear gradient of 5 to 100% acetonitrile at 0.3 mL min<sup>-1</sup> over 15 min.

Apo-Ybt eluted as diastereomers (1.0:3.5) at approximately 7.8 min (minor) and 8.3 min (major). HRMS (ESI+): exact mass calculated for C<sub>21</sub>H<sub>28</sub>N<sub>3</sub>O<sub>4</sub>S<sub>3</sub> [M+H]<sup>+</sup>, 482.1236 and for C<sub>21</sub>H<sub>29</sub>N<sub>3</sub>O<sub>4</sub>S<sub>3</sub> [M+2H]<sup>2+</sup>, 241.5655; found 482.1246 and 241.5664 for the minor isomer and 482.1239 and 241.5655 for the major isomer. In the original isolation and structural analysis of Ybt, Dreschel *et al* noted two apo-Ybt peaks which they characterized as epimers (a type of diastereomer) which are readily interconverted.<sup>64</sup> Our finding of two apo-Ybt peaks that coalesce into one Fe-Ybt complex<sup>63</sup> support the conclusions of Dreschel *et al.* that these peaks represent apo-Ybt epimers that are converted to one form by binding Fe<sup>3+</sup>.<sup>64</sup> Thus, we have combined these two peaks for our analyses of apo-Ybt. The isolated apo-Ybt was further analyzed by comparing the LC/MS data of the isolated material to authenticated apo-Ybt and was found to be identical (data not shown).

## PAR assay

Zn<sup>2+</sup> binding assays were performed using the metallochromic indicator dye 4-(2-pyridylazo)-resorcinol (PAR) (Sigma) and the methodology of Hunt *et al.*<sup>65</sup> PAR has a low absorbance at 490-500 nm in the absence of Zn<sup>2+</sup>; upon complexing with Zn<sup>2+</sup> the absorbance at this wavelength increases dramatically. To determine Zn<sup>2+</sup> chelating activity in *Y. pestis* supernatants, KIM6+ (Ybt<sup>+</sup>) and KIM6-2046.1 (Ybt<sup>-</sup>; *irp2::kan* mutant) were grown at 37°C in cPMH medium<sup>58</sup> supplemented with 40 mM MOPS pH7.5 for 30 h and supernatants harvested by pelleting cells. Cell densities of the two strains tested were



equivalent. Supernatant aliquots of 0.2 ml were filtered and used in the PAR assay (total volume of 0.5 ml). Reactions containing 40 mM HEPES-KOH, pH 7.4 and 3 (culture supernatants alone) or 5  $\mu$ M ZnCl<sub>2</sub> (*irp2::kan* mutant culture supernatants with or without 20  $\mu$ M apo-Ybt) were incubated for 15 min at room temperature before a PAR solution at pH 7.0 was added to a final concentration of 50  $\mu$ M. Residual Zn in cPMH is not sufficient to yield measurable chelation by PAR; consequently, any differences in Zn uptake between the two strains did not affect the assays, in which 3  $\mu$ M ZnCl<sub>2</sub> was added prior to incubation with PAR. After five min of incubation, the absorbance at 497 nm was measured with a Genesys5 spectrophotometer (Spectronic Instruments, Inc).

### Zn<sup>2+</sup>-binding studies of Ybt by <sup>1</sup>H NMR spectroscopy

Briefly, a 6.6 mM solution of Ybt was first prepared by dissolving 1.9 mg of apo-Ybt in 600  $\mu$ l of acetonitrile-*d*<sub>3</sub> (CD<sub>3</sub>CN) and analyzed by <sup>1</sup>H NMR spectroscopy. It was then treated with 3 equivalents of a solution of ZnCl<sub>2</sub> in CD<sub>3</sub>CN and allowed to stand for 3 min. The resulting mixture was also analyzed by <sup>1</sup>H NMR spectroscopy as previously described.<sup>66</sup>

### Cu<sup>2+</sup>, Fe<sup>3+</sup> and Zn<sup>2+</sup>-binding studies with Ybt

A 100 mM master stock solution of CuCl<sub>2</sub> was prepared by dissolving 0.60 g copper (II) chloride dihydrate powder (Sigma Aldrich) in 35.2 ml of ddH<sub>2</sub>O. A 2-fold dilution of this master stock solution yielded a 50 mM CuCl<sub>2</sub> stock solution, C<sub>1</sub>. A 100 mM master stock solution of FeCl<sub>3</sub> was prepared by dissolving 0.73 g iron-(III) hexahydrate in 27.0 ml mQH<sub>2</sub>O. A 2-fold dilution of this master stock solution yielded a 50 mM FeCl<sub>3</sub> stock solution, C<sub>2</sub>. A 1.00 M master stock solution of ZnCl<sub>2</sub> was prepared by dissolving 0.683 g ZnCl<sub>2</sub> in 5 ml of ddH<sub>2</sub>O. A 2-fold dilution of this master stock solution yielded a 500 mM ZnCl<sub>2</sub> stock solution, which was further subjected to a 10-fold dilution to yield a 50 mM ZnCl<sub>2</sub> stock solution, C<sub>3</sub>. To a cuvette containing 950  $\mu$ l of a 0.526 mM solution of Ybt in EtOH was added 50  $\mu$ l of H<sub>2</sub>O, C<sub>1</sub>, C<sub>2</sub> or C<sub>3</sub> corresponding to treatment with 0 or 5 equivalents of CuCl<sub>2</sub>, FeCl<sub>3</sub>, or ZnCl<sub>2</sub>, respectively. The resulting solution was gently mixed and allowed to stand for 2 min at room temperature before its absorbance was measured by UV-Vis spectroscopy from 200 to 900 nm in 10 nm increments as previously described.<sup>67</sup>

### Virulence testing

Construction and testing of potentially virulent strains was performed in a CDC-approved, BSL3 laboratory following Select Agent regulations using procedures approved by the University of Kentucky Institutional Biosafety Committee. All animal care and experimental procedures were approved by the University of Kentucky Institutional Animal Care and Use Committee.

For *Y. pestis* KIM6-2067( *ybtX*), KIM6-2197.2 ( *ybtX znuA*), KIM6-2070.3 (*ybtS::kan znuBC*), and KIM6-2196.4+ ( *zntA zur::kan*) mutants and KIM6-2197.4+ (YbtX<sup>+</sup> Znu<sup>-</sup>; *ybtX<sup>TP</sup>* [repaired *ybtX*] *znuA*), pCD1Ap was electroporated into each strain resulting in strains KIM5-2067(pCD1Ap) ( *ybtX*), KIM5-2197.2(pCD1Ap) ( *ybtX znuA*), KIM5-2070.3(pCD1Ap) (*ybtS::kan znuBC*), KIM5-2196.4(pCD1Ap)+ ( *zntA zur::kan*) and KIM5-2197.4(pCD1Ap)+ (*ybtX<sup>TP</sup> znuA*). Plasmid profiles, type III secretion phenotype and expression levels, and the CR phenotype were assessed as described previously.<sup>45, 57</sup> For

LD<sub>50</sub> studies, CR positive colonies were grown on a TBA slant overnight at 26°C, inoculated to an OD<sub>620</sub> of ~0.1 in HIB or HIB-FS supplemented with 50 µg Ap ml<sup>-1</sup>, 0.2% xylose, 2.5 mM CaCl<sub>2</sub> and 10 µM ZnCl<sub>2</sub> (except *ybtS::kan* and *zntA zur::kan* mutants which were grown without Zn<sup>2+</sup> supplementation) and grown at 26°C (for subcutaneous infections) or 37°C (for retro-orbital or intranasal infections) overnight. These cultures were diluted to an OD<sub>620</sub> of ~ 0.1 into the same medium, but without zinc supplementation, and grown at the same temperature for approximately two generations. 10-fold serially diluted bacterial suspensions<sup>45, 57</sup> of *ybtX*, *ybtX znuA*, *ybtX<sup>TP</sup> znuA*, and *zntA zur::kan* mutants were used for subcutaneous injections or intranasal infections of 6- to 8-week-old female Swiss Webster mice (Hsd::ND4). 10-fold serial dilutions of *ybtS::kan* and *ybtS::kan znuBC* mutants were injected into the retro-orbital plexus of Swiss Webster mice. For intranasal and retro-orbital infections, mice were sedated by intraperitoneal injection of a mixture of 100 µg of ketamine and 10 µg of xylazine per kg of body weight. Appropriate serial dilutions of suspensions used for injections were inoculated onto TBA plates containing Ap (50 µg ml<sup>-1</sup>) and 10µM ZnCl<sub>2</sub> (Zn supplementation was omitted for *ybtS::kan* and *zntA zur::kan* mutants) and colonies were counted after 2–3 days of incubation at 26°C. Mice were observed daily for 2 weeks and LD<sub>50</sub> values were calculated according to the method of Reed and Muench.<sup>68</sup>

### Macrophage infection and survival

Peritoneal macrophages were isolated from C57/B16 mice injected with 3 ml of thioglycolate medium as previously described.<sup>69</sup> Peritoneal and RAW264.7 macrophages were maintained in DMEM + 10% FBS. For infections, *Y. pestis* was grown overnight at 26°C in BHI, diluted 1:25 in fresh BHI, and grown at 26°C to an OD<sub>600</sub> ~1.0. Bacteria were diluted to desired concentration in 37°C DMEM+10%FBS and added to macrophages at a MOI=10. The infection was synchronized by centrifugation and extracellular bacteria were killed with 8 µg/ml gentamicin 20 min post-infection. One hour after gentamicin treatment, the medium was replaced with DMEM + 10% FBS containing gentamicin at a concentration of 2µg/ml (RAW264.7) or 1µg/ml (peritoneal). Intracellular bacterial numbers were determined by conventional CFU enumeration in triplicate as previously described.<sup>70</sup> Three independent trials with RAW274.6 cells were performed; one representative trial is shown. Patterns for RAW274.6 cells (growth) and peritoneal macrophages (survival but not growth) were typical for *Y. pestis*. The one trial with peritoneal macrophages confirmed the lack of a mutant phenotype similar to the RAW274.6 trials.

## Results

### The role of zinc homeostasis in the lethal progression of bubonic and pneumonic plague in mice

Previously, we demonstrated the critical role of *Y. pestis* Zn<sup>2+</sup> uptake via a HMWP2 product and the ZnuABC transporter for the lethal progression of septicemic plague in mice using an *irp2::kan znuBC* mutant (KIM5-2077.7(pCD1Ap). Ybt biosynthetic mutants cannot be used in bubonic and pneumonic plague models since this mutation alone causes dramatic virulence losses (*e.g.*, *irp2* mutations show >5 × 10<sup>5</sup>-fold and 790-fold virulence losses, respectively).<sup>57</sup>

However, previous studies showed that YbtX is not required for Fe<sup>3+</sup> uptake but rather for Ybt-dependent Zn<sup>2+</sup> uptake;<sup>45, 71</sup> thus we used single *ybtX* or *znuA* mutants, a double *ybtX znuA* mutant and a *ybtX<sup>TP</sup>* (repaired *ybtX*) *znuA* mutant carrying the pCD1Ap virulence plasmid that encodes a type three secretion system [KIM5-2067(pCD1Ap) (*ybtX*) or KIM5-2197(pCD1Ap)+ (*znuA*), KIM5-2197.2(pCD1Ap) (*ybtX znuA*) and KIM5-2197.4(pCD1Ap)+ (*ybtX<sup>TP</sup> znuA*), respectively] to assess the role of these systems in Zn<sup>2+</sup> acquisition in mouse models of bubonic and pneumonic plague. Outbred Swiss-Webster mice were infected subcutaneously or intranasally to mimic bubonic or pneumonic plague, respectively, and observed for two weeks. As expected, the *ybtX* mutant retained high lethality similar to the parent strain and the *znuB* mutant (Table 1 and Ref<sup>59, 72</sup>). However, the double *ybtX znuA* mutant was essentially avirulent in mouse models of bubonic and pneumonic plague (Table 1). The *ybtX znuA* mutant showed an ~10<sup>6</sup>-fold loss of virulence compared to the *ybtX* strain in the mouse model of bubonic plague. Strikingly, intranasal instillation with 1.5 × 10<sup>6</sup> cells (highest infectious dose used) of the double mutant did not cause any disease symptoms, suggesting complete attenuation. The virulence of the *ybtX znuA* mutant was restored in both models when the chromosomal *ybtX* mutation was repaired (*ybtX<sup>TP</sup>*; Table 1). These data show that Zn<sup>2+</sup> acquisition is essential for the progression of both bubonic and pneumonic plague. While individually the *Y. pestis* YbtX and ZnuABC transporters are dispensable, mutation of both systems causes essentially complete attenuation in both bubonic and pneumonic plague mouse models .

While bacteria require Zn for growth, elevated levels of Zn can also be toxic to bacteria and phagocytes have evolved to use Zn as part of their antimicrobial arsenal.<sup>73-77</sup> Therefore, the ability to avoid Zn toxicity via Zn<sup>2+</sup> efflux has also been shown as an important virulence factor in several bacteria.<sup>76, 78-80</sup> *Y. pestis* is a facultative intracellular pathogen and has been shown to survive in macrophages, and to a lesser extent in neutrophils.<sup>81-85</sup> While bioinformatics identified several systems predicted to be involved in Zn<sup>2+</sup> efflux in the *Y. pestis* KIM10+ genome,<sup>59</sup> their role in virulence and in preventing Zn toxicity has not been determined. Y410 encodes a protein with a high degree of similarity (65% identity over 709 amino acid residues) to ZntA, a P-type ATPase that is a primary Zn<sup>2+</sup> exporter in *E. coli*.<sup>86</sup> Transcription of *Y. pestis zntA* was detected in the lymph nodes of plague-infected rats but not during colonization of fleas,<sup>87, 88</sup> suggesting that zinc efflux by ZntA may be important during bubonic plague. Deletion of *zntA* (KIM6-2196.1+) led to drastically increased Zn sensitivity *in vitro* compared to the parent strain (Fig. 1) suggesting that ZntA plays an important role in preventing Zn toxicity in *Y. pestis*. Another mechanism to prevent Zn toxicity in bacteria occurs via transcriptional repression of genes encoding Zn<sup>2+</sup> importers by Zur.<sup>2, 89</sup> In *Y. pestis*, inactivation of Zur leads to increased expression of *znuABC* genes<sup>59, 90</sup> which causes unregulated Zn<sup>2+</sup> uptake and could result in increased susceptibility to toxic Zn levels. However a *zur::kan* mutation (strain KIM6-2078) did not affect sensitivity of *Y. pestis* to high levels of Zn<sup>2+</sup> (Fig. 1). The sensitivity of a double *zntA zur::kan* mutant (KIM6-2196.4+) to Zn was similar to that of the *zntA* mutant (Fig. 1). These results suggest that ZntA is important in preventing Zn toxicity while Zur is not – at least *in vitro*.

To assess the *in vivo* role of ZntA and Zur, we preformed subcutaneous (bubonic plague) and intranasal (pneumonic plague) infections using the double *zntA zur::kan* mutant transformed with pCD1Ap to restore potential virulence [KIM5-2196.45(pCD1Ap)]. The

double mutant had an LD<sub>50</sub> similar to that for the parent Zur<sup>+</sup> ZntA<sup>+</sup> strain [KIM5(pCD1Ap) +] in the bubonic plague model (Table 1 and Ref <sup>57</sup>). In the mouse model of pneumonic plague, the double *zntA zur::kan* mutant showed only a slight (~4-fold) increase in the LD<sub>50</sub> compared to that of the parent strain (Table 1 and Ref <sup>57</sup>).

Since the Zn toxicity host defense occurs in phagocytic cells,<sup>73-77</sup> we tested the survival of the *zntA zur::kan* mutant in RAW274.6 and peritoneal macrophages. Over a 24-h period post-infection, the parent (ZntA<sup>+</sup> Zur<sup>+</sup> KIM6+) strain and the *zntA zur::kan* mutant (KIM6-2196.4) had nearly identical invasion, survival and growth characteristics in both RAW274.6 and peritoneal macrophages (Fig. 2). Together, these results suggest that *Y. pestis* either does not face toxic Zn levels during mammalian infection or that other Zn<sup>2+</sup> exporter(s) or Zn<sup>2+</sup> homeostasis mechanisms compensate for the loss of ZntA and Zur in *Y. pestis*.

### The salicylate synthase YbtS is irrelevant for Zn-dependent growth *in vitro* but critical for virulence of a *znu* mutant during septicemic plague

Previously, we showed that HMWP2 and YbtU (a reductase) are both required for Ybt biosynthesis and for growth under low Zn<sup>2+</sup> conditions in a *znu* background.<sup>45</sup> Here we examine the effect of three other mutations that prevent Ybt biosynthesis, *ybtE*, *irp2 S52* and *ybtS::kan*, on the growth, under low Zn<sup>2+</sup> conditions, of a *znuBC Y. pestis* strain. YbtE adenylates salicylate for loading onto residue S52 of HMWP2 and both the *ybtE znuA* and the *irp2 S52 znuA* double mutants (KIM6-2056.2 and KIM6-2046.9, respectively) were unable to grow in cPMH2 supplemented with 0.6 μM ZnCl<sub>2</sub> and 1 μM FeCl<sub>3</sub> (Fig. S1). In contrast, the *ybtS::kan* mutation in KIM6-2070.1 that inactivates the salicylate synthase YbtS did not affect growth in the *znuBC* mutant background (KIM6-2070.3) under similar conditions (Fig. 3A).

Most mutations that abrogate Ybt biosynthesis cause reduced transcription of the *ybt* operons and thus lower expression of Ybt biosynthetic and transport enzymes. However in the *ybtS::kan* mutant, the expression level of the *ybt* genes is normal.<sup>63, 91, 92</sup> Previously, we speculated that a Ybt-like molecule produced by the remaining Ybt biosynthetic module in a *ybtS::kan* mutant was responsible for transcriptional activation of *ybt* genes but was not able to stimulate growth under iron-deficient conditions.<sup>63</sup> It is possible that this Ybt-like molecule also binds Zn<sup>2+</sup> and thus permits the growth of the *ybtS::kan znuBC* mutant. However, supernatants from a *ybtS::kan* and *irp2::kan* (negative control) cultures failed to stimulate the growth of the *irp2::kan psn znuBC* mutant (KIM6-2077.18) in contrast to the growth stimulation observed in supernatant from the Ybt<sup>+</sup> parent KIM6+ strain (Fig. 3B)

We next tested the virulence of the *ybtS::kan znuBC Y. pestis* mutant in a septicemic mouse model of plague. Since the *ybtS::kan znuBC* mutant had a growth phenotype similar to the *znuBC* mutant (KIM6-2077+) *in vitro*, we expected this double mutant to have the same fully virulent phenotype as the single *znuBC* mutant [KIM5-2197(pCD1Ap)]. Surprisingly, the *ybtS::kan znuBC* mutant transformed with pCD1Ap [KIM5-2070.3(pCD1Ap)] was essentially avirulent with an ~10<sup>6</sup>-fold loss of virulence compared to the *znuBC* mutant (Table 1) – a virulence defect similar to that of an *irp2::kan znuBC* mutant [KIM5-2077.7(pCD1Ap)].<sup>45</sup>

## Investigation of the siderophore-dependent mechanisms of Zn<sup>2+</sup> acquisition in *Y. pestis*

Our earlier study showed that loss of Ybt biosynthesis ( *irp2* or *irp2::kan* mutations) in combination with a *znuBC* mutation caused an *in vitro* growth defect under low-Zn<sup>2+</sup> conditions and a significant reduction in virulence in a mouse septicemic plague model. Supplementation of a *irp2 psn znuBC* culture with apo-Ybt stimulated growth *in vitro*.<sup>45</sup> The Henderson research group had previously shown that Ybt binds Cu<sup>2+</sup>.<sup>93</sup> In a more recent study, this same research group found that purified Ybt also binds Cr<sup>3+</sup>, Co<sup>2+</sup> and Ni<sup>2+</sup> but not Zn<sup>2+</sup> or Mn<sup>2+</sup>.<sup>94</sup> However, it is possible that *Y. pestis* produces isomeric form of Ybt with different metal binding properties. Note that two isomers of the pyochelin siderophore are transported by different transport systems in *P. aeruginosa* and *P. fluorescens*.<sup>95</sup> Therefore, we have investigated whether Ybt purified from *Y. pestis* directly binds Zn<sup>2+</sup> and other possible roles of Ybt biosynthesis in Zn<sup>2+</sup> uptake by *Y. pestis*.

In *Y. pestis*, the Ybt siderophore has a dual function as a Fe<sup>3+</sup> carrier and as a signaling molecule that activates transcription of *ybt* operons including *ybtPQXS*. To determine whether the role of the siderophore is simply to stimulate expression of YbtX, we constructed a *ybtX* clone whose expression is controlled by the *znuA* promoter and examined the low-Zn<sup>2+</sup> growth response of a double *irp2 znuA* mutant (KIM6-2197.1) carrying this clone. Although the level of YbtX expressed was similar to that of a Ybt-producing strain, the growth of the mutant strain was not restored under these conditions (Fig. 4). Thus Ybt biosynthesis does not enhance Zn<sup>2+</sup> uptake simply by increased expression of YbtX.

However, this does not eliminate the possibility that YbtA-Ybt activates transcription of an unidentified transport component that acts in conjunction with YbtX. To address this, we used the IPTG-inducible YbtA expression vector, pQEYbtA which we have previously shown activates transcription from the *ybtPQXS* promoter 42-fold even in the absence of the Ybt siderophore, similar to other overexpressed AraC-type transcriptional regulators.<sup>92</sup> The double *irp2 znuA* mutant failed to grow in cPMH2 supplemented with 1 μM FeCl<sub>3</sub>, 0.6 μM ZnCl<sub>2</sub>, and 1 mM IPTG, whether this mutant carried the pQE30 vector or pQEYbtA (Fig. S2). Thus our data support a model in which Ybt is not simply serving as a signaling molecule to stimulate expression of YbtX and/or any additional putative Zn<sup>2+</sup> transport components.

To test the ability of culture supernatants from a Ybt-producing strain (KIM6+) and a Ybt biosynthetic (*irp2::kan*) mutant (KIM6-2046.1) to chelate Zn<sup>2+</sup>, we used the PAR assay which has been widely used for the identification of Zn-binding activity by a number of proteins. PAR is calculated to form 1:1 and 2:1 complexes with Zn<sup>2+</sup> with stepwise affinity constants of  $4.0 \times 10^6$  and  $5.5 \times 10^5 \text{ M}^{-1}$ , which corresponds to an overall conditional stability constant of  $2 \times 10^{12} \text{ M}^{-1}$ .<sup>65</sup> Therefore, the PAR assay can be used for monitoring Zn<sup>2+</sup> binding in the range of nM to pM. To measure compounds with high affinity for binding Zn<sup>2+</sup>, a PAR/Zn ratio of >10 was used to ensure the presence of only PAR<sub>2</sub>-Zn complexes in the assay. If Ybt binds Zn<sup>2+</sup>, it will remove free Zn<sup>2+</sup> from the assay and reduce Zn<sup>2+</sup> binding by PAR as measured by a reduction in absorbance at 497 nm. Indeed the culture supernatant from the Ybt-producing strain had a significantly higher Zn<sup>2+</sup>-chelating activity compared to the supernatant from the *irp2::kan* mutant that is unable to

produce Ybt (1.6-fold), and a 2.9-fold difference from uninoculated cPMH (Fig. 5A). Thus our data demonstrate the presence of a ligand(s) with high affinity to  $Zn^{2+}$  in the culture supernatant from the Ybt producing strain of *Y. pestis*.

Although the higher  $Zn^{2+}$ -binding activity detected in the Ybt-producing supernatant by the PAR assay (Fig. 5A) suggests that Ybt binds  $Zn^{2+}$ , Koh *et al.* found no evidence for  $Zn^{2+}$  binding by *E. coli* apo-Ybt by MS/MS analysis.<sup>94</sup> We have purified apo-Ybt from *Y. pestis* to further analyze its potential for  $Zn^{2+}$  binding. Addition of apo-Ybt to the *irp2::kan* culture supernatant did not change its  $Zn^{2+}$ -binding activity as determined by the PAR assay (Fig. 5B), a puzzling result since supernatants from Ybt-producing cells showed increased  $Zn^{2+}$ -binding activity compared to culture supernatants from a strain unable to synthesize Ybt. Consequently, we used additional approaches to test for  $Zn^{2+}$ -binding activity by Ybt. Similar to the results of Koh *et al.*,<sup>94</sup> our MS analysis of HPLC-purified apo-Ybt from *Y. pestis* showed no evidence of  $Zn^{2+}$  binding (data not shown). Addition of  $Fe^{3+}$  or  $Cu^{2+}$  significantly altered the UV-visible spectra compared to apo-Ybt (Fig. 6). In contrast, the absorption spectra of apo-Ybt compared to apo-Ybt plus  $Zn^{2+}$  were nearly identical (Fig. 6). While some small  $Zn^{2+}$ -binding molecules display differences in spectra upon  $Zn^{2+}$  binding,<sup>96</sup> our experience with chalcones indicates that this does not always occur.<sup>67</sup> To further assess possible  $Zn^{2+}$ -binding by Ybt,  $^1H$  NMR spectra were performed. Using this approach, we found no significant differences in the  $^1H$  NMR spectra of apo-Ybt and apo-Ybt plus Zn (Fig. 7). While our data indicate that purified *Y. pestis* Ybt does not directly bind  $Zn^{2+}$  in biochemical assays, it also suggests that Ybt or a modified Ybt participates in or promotes Zn-binding activity in culture supernatants and is involved in Zn acquisition in *Y. pestis*.

## Discussion

Mammals respond to bacterial infections by increasing  $Zn^{2+}$  sequestration in an attempt to withhold  $Zn^{2+}$  from the invading pathogen (nutritional immunity) and a number of bacterial pathogens lose virulence when  $Zn^{2+}$  transporters are mutated, especially ZnuABC.<sup>13-16, 97</sup> Previously we found that a *Y. pestis znuBC* mutant retained high virulence in both bubonic and pneumonic models of plague, suggesting that other  $Zn^{2+}$  transporter(s) compensated for the loss of ZnuABC. Mutation of a number of other cation transporters failed to identify any as  $Zn^{2+}$  transporters.<sup>59, 98, 99</sup> However, we found that an *irp2* mutation (causing loss of Ybt synthesis) in a *Y. pestis znuBC* background has an extreme *in vitro* growth defect under low- $Zn^{2+}$  conditions and was highly attenuated ( $> 4 \times 10^5$ -fold virulence loss) in a mouse model of septicemic plague. We further found that YbtX, a member of the Major Facilitator Superfamily, is involved in  $Zn^{2+}$  acquisition. These results led us to suggest that Ybt might serve as a zincophore as well as a siderophore.<sup>45</sup>

While mutations that affect either transport or synthesis of Ybt cause nearly complete loss of virulence or high attenuation in bubonic and pneumonic models of plague, a *ybtX* mutation does not affect  $Fe^{3+}$  uptake via the Ybt system.<sup>57, 71</sup> Consequently, here we used a *Y. pestis ybtX znuA* mutant [KIM5-2197.2(pCD1Ap)] to demonstrate nearly complete virulence loss in mouse models of bubonic and pneumonic plague due to these two mutations. Like the single *znuBC* [in KIM5-2077(pCD1Ap)+]<sup>59</sup> and *znuA* mutations [KIM5-2197(pCD1Ap)]

+) (Table 1), a single *ybtX* mutation [in KIM5-2197(pCD1Ap)] did not significantly affect virulence in either disease model (Table 1 and Ref <sup>72</sup>). For a number of pathogens, including *Y. pestis*, the importance of specific Fe<sup>3+</sup> and 2<sup>+</sup> and Mn<sup>2+</sup> transporters in disease progression or intracellular vs extracellular residence varies by organ system.<sup>57, 97, 100-102</sup> In contrast, these two Zn<sup>2+</sup> transporters in *Y. pestis* appear to serve essential but overlapping or redundant functions *in vivo* with loss of both systems required to significantly affect virulence (Table 1 and Ref <sup>59, 72</sup>).

Since *ybtX* is highly expressed in the lungs during pneumonic infection <sup>103</sup>, Pechous *et al.*<sup>72</sup> recently tested a *Y. pestis ybtX* mutant in a mouse model of pneumonic plague. They found that this mutation does not affect lung colonization or bacterial dissemination but reduces inflammation in the lungs likely by reducing expression of proinflammatory cytokines IL-6 and IL-17 and chemokines CXCL1 and CCL2 which decrease neutrophil infiltration. They speculated that YbtX reduces Zn levels in the lungs causing increased inflammation, a property of Zn<sup>2+</sup> deficiency.<sup>6, 15, 72, 75</sup> Thus YbtX appears to serve two *in vivo* roles – contributing to bacterial Zn<sup>2+</sup> acquisition and to inflammation in the lung.

While sequestration of host Zn<sup>2+</sup> is a key nutritional immunity factor, there is recent evidence for excess Zn<sup>2+</sup> having a significant antimicrobial role in controlling bacterial infections. Mutation of various Zn<sup>2+</sup> exporters in several bacteria decrease survival in phagocytic cells and sometimes also affects the development of disease in mice.<sup>75</sup> Here we demonstrated that mutation of *zntA*, encoding a major Zn<sup>2+</sup> exporter in *E. coli*, but not in *zur*, encoding a Zn-responsive transcriptional regulator, increased the sensitivity of *Y. pestis* to excess Zn *in vitro* (Fig. 1). However, a *Y. pestis zntA zur::kan* double mutant [KIM5-2196.4([CD1Ap)] retained high virulence in mouse models of bubonic and pneumonic plague (Table 1) and resistance to killing by macrophages (Fig. 2). Although this suggests that *Y. pestis* does not encounter toxic levels of Zn<sup>2+</sup> during mammalian infection, it is also possible that other putative Zn<sup>2+</sup> exporters (*e.g.*, ZitB, ZntB and/or FieF) function *in vivo* to prevent toxicity.

Shortly after we suggested that Ybt might be a zincophore, the Henderson research group used MS analysis to demonstrate that Ybt purified from *E. coli* binds Cu<sup>2+</sup>, Co<sup>2+</sup>, Cr<sup>2+</sup>, Ga<sup>3+</sup> and Ni<sup>2+</sup> but not Mn<sup>2+</sup> or Zn<sup>2+</sup>.<sup>94</sup> Here we examined the ability of apo-Ybt purified from *Y. pestis* to bind Zn<sup>2+</sup> using MS (data not shown), <sup>1</sup>H NMR (Fig. 7), UV-Vis spectra (Fig. 6), and a Zn<sup>2+</sup>-binding PAR assay (Fig. 5B). Results from all of these methods supported the original conclusion of Koh *et al.*<sup>94</sup> that apo-Ybt does not directly bind Zn<sup>2+</sup> with significant affinity. These results are puzzling in light of our findings that: (1) Ybt does not appear to simply act as a signal molecule to increase expression of YbtX or other putative components of the Ybt-dependent Zn<sup>2+</sup> transport system (Fig. 4 and S2); (2) the addition of apo-Ybt to the *irp2::kan psn znu* mutant (KIM6-2077.18) stimulates growth under low-Zn<sup>2+</sup> conditions;<sup>45</sup> and (3) supernatant from a Ybt-producing strain had a higher Zn<sup>2+</sup>-binding activity by the PAR assay than supernatant from a non-producing strain (Fig. 5A). Detection by PAR indicates this unidentified Zn<sup>2+</sup>-binding compound has a higher affinity for Zn<sup>2+</sup> than PAR ( $2 \times 10^{12} \text{ M}^{-1}$ ).

Based on all these results, we favor two alternative models for  $Zn^{2+}$  acquisition using components of the Ybt system. First, Ybt plus a second compound (for convenience, tentatively termed YbtZ) together might bind  $Zn^{2+}$  (Fig. 8). Since addition of apo-Ybt to the growth medium stimulates growth of the double  $Zn^{2+}$  transport mutant, we expected that addition of apo-Ybt to the Ybt-negative culture supernatant would allow this interaction and cause increased  $Zn^{2+}$ -binding activity by the PAR assay. However, addition of apo-Ybt to the *irp2::kan* (KIM6-2046.1) culture supernatant did not change its  $Zn^{2+}$ -binding activity (Fig. 5B). Nonetheless, this scenario is still possible. Lability of the putative YbtZ in the absence of interaction with Ybt would explain why addition of apo-Ybt to a Ybt-negative culture supernatant did not restore  $Zn^{2+}$  binding. In this model secreted Ybt complexes with secreted YbtZ to form a zincophore (tentatively termed Zbt) (Fig. 8). In the second model, Ybt is enzymatically modified into a form that binds  $Zn^{2+}$ . In this model, conversion of Ybt to a  $Zn^{2+}$ -binding molecule (also termed Zbt) occurs after secretion (Fig. 8) since a *irp2::kan psn znuBC* mutant showed growth stimulation by external apo-Ybt. The *psn* mutation would prevent uptake and intracellular conversion of Ybt.<sup>45, 104</sup> Previously, we reported that a *psn znuBC* mutant grows better than a *znuBC* mutant under  $Zn^{2+}$ -deficient conditions suggesting that the lack of a Psn receptor allows all available Ybt to be used for  $Zn^{2+}$  uptake.<sup>45</sup> These results fit with both models. However, isolation and identification of the putative Zbt zincophore (either Ybt-YbtZ or a modified Ybt) is needed to support either of these two proposed models. Although we have found that the Ybt synthesis-dependent Zn-binding activity is extracted into ethyl acetate (data not shown), we have yet to isolate the putative zincophore.

The Ybt-like compound produced by the *ybtS::kan* mutant (KIM6-2070.1; Fig. 3A and Ref<sup>63</sup>) remains elusive. We have not detected this compound in culture supernatants of the *ybtS::kan* mutant (Fig. 3B) which could indicate the compound is cell associated similar to some other siderophores.<sup>105-108</sup> Bioinformatics revealed several *Y. pestis* genes that could be involved in biosynthesis of a membrane-bound siderophore. In *Y. pestis*, *y2236* encodes a putative fatty acid CoA ligase orthologous to *V. harveyi* AebG, which is required for the synthesis of membrane-bound amphi-enterobactin.<sup>106</sup> Micacocidin, produced by a *Pseudomonas* sp. and *Ralstonia solanacearum*, binds  $Zn^{2+}$  and  $Fe^{3+}$  and has a structure very similar to that of Ybt with an additional pentyl chain on the salicylate moiety which we speculate could lead to cell association. This biosynthetic pathway does not use salicylate as a precursor<sup>54, 55, 109, 110</sup> and *Y. pestis* has a truncated gene (*y3406*) that encodes some domains of the polyketide synthase MicC from *Ralstonia solanacearum*, which initiates biosynthesis of micacocidin. MicC uses acyl carrier protein-tethered hexanoic acid as a precursor resulting in production of a hydrophobic pentyl chain linked to the salicylate moiety.<sup>109</sup> We speculated that a AebG-like or a MicC-related enzyme may initiate biosynthesis of a hydrophobic siderophore using the remaining Ybt biosynthetic machinery. However, neither the *y4306 ybtS::kan znu* (KIM6-2070.4) nor the *y2236 ybtS::kan znuBC* (KIM6-2070.5) triple *Y. pestis* mutants had a growth defect similar to that of an *irp::kan znuBC* double mutant (KIM6-2077.7) under low-Zn growth conditions (Fig. S3). While the pathway (and enzymes) for synthesis of the proposed Ybt-like molecule mutant remains to be identified, this compound seems unlikely to have a significant biological role



during animal infections. The *ybtS::kan znuBC* double mutant [KIM5-2070.3(pCD1Ap)] was essentially avirulent in the mouse model of septicemic plague (Table 1).

The PAR assay detected a residual  $Zn^{2+}$ -binding activity in the Ybt-negative culture supernatant - a 1.8-fold difference compared to uninoculated cPMH (Fig. 5A). Although this suggests that the *irp2::kan* mutant produces a secreted, high-affinity  $Zn^{2+}$ -binding compound, we have no evidence that this ligand plays a role in  $Zn^{2+}$  acquisition. Recently, two different extracellular  $Zn^{2+}$ -binding compounds have been characterized. Wang *et al.*<sup>111</sup> demonstrated that a 117-residue protein (YPK\_3549) of *Yersinia pseudotuberculosis* binds  $Zn^{2+}$ . This protein, which was designated YezP (*Yersinia* extracellular  $Zn^{2+}$ -binding protein) is secreted by a type VI secretion system. Mutation of the secretion system reduced intracellular Zn levels *in vitro* and a *yezP znu Y. pseudotuberculosis* double mutant showed a significant loss of virulence via orogastric infection of mice.<sup>111</sup> *Y. pestis* encodes homologues of the type VI secretion system and *yezP* (*y3657* in *Y. pestis*). However, Y3657 is unlikely to be responsible for the residual  $Zn^{2+}$ -binding activity in the *znu irp2* mutant since our preliminary isolation studies of the unidentified  $Zn^{2+}$ -binding ligand indicates it is <3 kDa, resistant to boiling and proteinase K treatments (data not shown). In addition, we have no evidence that *y3657* plays a  $Zn^{2+}$  acquisition role in *Y. pestis*. The *irp2::kan znu* and *ybtX znuA Y. pestis* double mutants are growth defective with 0.6  $\mu$ M Zn supplementation (Fig. S3 and Ref<sup>45</sup>) suggesting no additional high affinity  $Zn^{2+}$  uptake system is functional *in vitro*. Also, a *y3657::kan znuBC* double mutant (KIM6-2202.1+) had an *in vitro* growth phenotype similar to the *znu* mutant (data not shown). Thus, in *Y. pestis*, at least *in vitro*, Y3657 does not seem to be an independent  $Zn^{2+}$  importer or to work with the Ybt system for  $Zn^{2+}$  uptake.

The second system is a metallophore (staphylophine) and ABC transporter in *Staphylococcus aureus* that is involved in  $Co^{3+}$ ,  $Cu^{2+}$ ,  $Fe^{3+}$ ,  $Ni^{2+}$  and  $Zn^{2+}$  acquisition. CntKLM enzymes synthesize the small metallophore while CntE exports it and CntA-F import the metal complex.<sup>112, 113</sup> The *Y. pestis* KIM genome has genes with significant similarities for the biosynthesis of the metallophore.<sup>112</sup> Consequently, the Ybt-independent  $Zn^{2+}$ -binding compound could correspond to staphylophine. However, our current evidence does not support an important *in vitro* or *in vivo*  $Zn^{2+}$  acquisition role for the staphylophine system in *Y. pestis*. Our *irp2::kan znuBC* and *ybtX znuA* double mutants are growth defective under low  $Zn^{2+}$  growth conditions *in vitro* and our *ybtX znuA* double mutant is essentially avirulent in bubonic and pneumonic plague mouse models (Table 1 and Ref<sup>45</sup>). We have also examined the *Y. pestis* ABC transporter (*y2842-y2837*) encoded upstream of the staphylophine biosynthetic genes (*y2836-y2834*). In a *znuBC* background, mutation of *y2842*, which encodes the periplasmic binding protein for the ABC transporter, did not further affect growth under Zn-deficient conditions.<sup>59</sup> In addition, the second gene, encoding a permease, has undergone a frameshift mutation, making it unlikely to be functional.<sup>114</sup> Finally, *Y. pestis* KIM lacks *cntK* whose protein product converts L-histidine to D-histidine, the first step in staphylophine synthesis.<sup>112, 113</sup> Thus the functionality of this system in *Y. pestis* is uncertain.

## Conclusions

This study has demonstrated that  $Zn^{2+}$  acquisition by *Y. pestis* is critical for the progression of bubonic and pneumonic plague. We have provided additional evidence that the Ybt siderophore does not directly bind  $Zn^{2+}$  but instead we suggest that a modified Ybt molecule or Ybt plus a second compound (YbtZ) may be the zincophore (Zbt). Although additional  $Zn^{2+}$ -binding compounds are encoded or expressed by *Y. pestis*, the Znu and YbtX systems remain the only two proven high-affinity  $Zn^{2+}$  importers functional *in vitro* or *in vivo*. Finally, while *zntA* and *zntA zur::kan* mutants had increased Zn sensitivity *in vitro* compared to their  $ZntA^+ Zur^+$  parent, the *zntA zur::kan* mutant retained high virulence in mouse models of bubonic and pneumonic plague. This suggests that *Y. pestis* either does not encounter toxic Zn levels during intracellular residence or other Zn efflux systems are used *in vivo* to prevent Zn toxicity,

## Supplementary Material

Refer to Web version on PubMed Central for supplementary material.

## Acknowledgments

This work was supported by Public Health Services Grant R01 AI33481 from the US National Institutes of Health and by startup funds from the University of Kentucky (to S.G.-T.). M.B.L. and T.T.V. were supported by Public Health Services grant R21 AI119557 from the US National Institutes of Health.

## References

1. Andreini C, Banci L, Bertini I, Rosato A. Zinc through the three domains of life. *J Proteome Res.* 2006; 5:3173–3178. [PubMed: 17081069]
2. Hantke K. Bacterial zinc uptake and regulators. *Curr Opin Microbiol.* 2005; 8:196–202. [PubMed: 15802252]
3. Katayama A, Tsujii A, Wada A, Nishino T, Ishihama A. Systematic search for zinc-binding proteins in *Escherichia coli*. *Eur J Biochem.* 2002; 269:2403–2413. [PubMed: 11985624]
4. Vallee BL, Falchuk KH. The biochemical basis of zinc physiology. *Physiol Rev.* 1993; 73:79–118. [PubMed: 8419966]
5. Corbin BD, Seeley EH, Raab A, Feldmann J, Miller MR, Torres VJ, Anderson KL, Dattilo BM, Dunman PM, Gerads R, Caprioli RM, Nacken W, Chazin WJ, Skaar EP. Metal chelation and inhibition of bacterial growth in tissue abscesses. *Science.* 2008; 319:962–965. [PubMed: 18276893]
6. Rink L, Haase H. Zinc homeostasis and immunity. *Trends Immunol.* 2007; 28:1–4. [PubMed: 17126599]
7. Foote JW, Delves HT. Albumin bound and  $\alpha_2$ -macroglobulin bound zinc concentrations in the sera of healthy adults. *J Clin Pathol.* 1984; 37:1050–1054. [PubMed: 6206098]
8. Hood MI, Skaar EP. Nutritional immunity: transition metals at the pathogen-host interface. *Nat Rev Microbiol.* 2012; 10:525–537. [PubMed: 22796883]
9. Liuzzi JP, Lichten LA, Rivera S, Blanchard RK, Aydemir TB, Knutson MD, Ganz T, Cousins RJ. Interleukin-6 regulates the zinc transporter Zip14 in liver and contributes to the hypozincemia of the acute-phase response. *Proc Natl Acad Sci U S A.* 2005; 102:6843–6848. [PubMed: 15863613]
10. Weinberg ED. Infectious diseases influenced by trace element environment. *Ann N Y Acad Sci.* 1972; 199:274–284. [PubMed: 4506512]

11. Rahuel-Claremont, S., Dunn, MF. Copper and Zinc in Inflammatory and Degenerative Diseases. Rainsford, KD. Milanino, R. Sorenson, RJ., Velo, GP., editors. Kluwer Academic Publisher; 1998. p. 47-59.
12. Sohnle PG, Hunter Michael J, Hahn B, Chazin Walter J. Zinc reversible antimicrobial activity of recombinant calprotectin (migration inhibitory factor - related proteins 8 and 14). *J Infect Dis*. 2000; 182:1272–1275. [PubMed: 10979933]
13. Becker KW, Skaar EP. Metal limitation and toxicity at the interface between host and pathogen. *FEMS Microbiol Rev*. 2014; 38:1235–1249. [PubMed: 25211180]
14. Diaz-Ochoa V, Jellbauer S, Klaus S, Raffatellu M. Transition metal ions at the crossroads of mucosal immunity and microbial pathogenesis. *Front Cell Infect Microbiol*. 2014; 4:2. [PubMed: 24478990]
15. Rehder, D., Black, RE., Bornhorst, J., Dietert, RR., DiRita, VJ., Navarro, M., Perry, RD., Rink, L., Skaar, EP., Soares, MCP., Thiele, DJ., Wang, F., Weiss, G., Wessels, I. Trace Metals and Infectious Diseases. Nriagu, JO., Skaar, EP., editors. Vol. ch. 13. MIT Press; Cambridge, MA USA: 2015. p. 199-226.
16. Caveat, JS., Perry, RD., Brunke, S., Darwin, KD., Fierke, CA., Imlay, JA., Murphy, MEP., Schryvers, AB., Thiele, DJ., Weiser, JN. Trace Metals and Infectious Diseases. Nriagu, JO., Skaar, EP., editors. Vol. ch. 7. MIT Press; Cambridge, MA USA: 2015. p. 99-122.
17. Ammendola S, Pasquali P, Pistoia C, Petrucci P, Petrarca P, Rotilio G, Battistoni A. High-affinity Zn<sup>2+</sup> uptake system ZnuABC is required for bacterial zinc homeostasis in intracellular environments and contributes to the virulence of *Salmonella enterica*. *Infect Immun*. 2007; 75:5867–5876. [PubMed: 17923515]
18. Bayle L, Chimalapati S, Schoehn G, Brown J, Vernet T, Durmort C. Zinc uptake by *Streptococcus pneumoniae* depends on both AdcA and AdcAII and is essential for normal bacterial morphology and virulence. *Mol Microbiol*. 2011; 82:904–916. [PubMed: 22023106]
19. Campoy S, Jara M, Busquets N, Pérez de Rozas AM, Badiola I, Barbé J. Role of the high-affinity zinc uptake *znuABC* system in *Salmonella enterica* serovar typhimurium virulence. *Infect Immun*. 2002; 70:4721–4725. [PubMed: 12117991]
20. Cerasi M, Ammendola S, Battistoni A. Competition for zinc binding in the host-pathogen interaction. *Front Cell Infect Microbiol*. 2013; 3:108. [PubMed: 24400228]
21. Cerasi M, Liu JZ, Ammendola S, Poe AJ, Petrarca P, Pesciaroli M, Pasquali P, Raffatellu M, Battistoni A. The ZupT transporter plays an important role in zinc homeostasis and contributes to *Salmonella enterica* virulence. *Metallomics*. 2014; 6:845–853. [PubMed: 24430377]
22. Corbett D, Wang J, Schuler S, Lopez-Castejon G, Glenn S, Brough D, Andrew PW, Cavet JS, Roberts IS. Two zinc uptake systems contribute to the full virulence of *Listeria monocytogenes* during growth *in vitro* and *in vivo*. *Infect Immun*. 2012; 80:14–21. [PubMed: 22025520]
23. Dahiya I, Stevenson RMW. The ZnuABC operon is important for *Yersinia ruckeri* infections of rainbow trout, *Oncorhynchus mykiss* (Walbaum). *Journal of Fish Diseases*. 2010; 33:331–340. [PubMed: 20070462]
24. Davis LM, Kakuda T, DiRita VJ. A *Campylobacter jejuni znuA* orthologue is essential for growth in low-zinc environments and chick colonization. *J Bacteriol*. 2009; 191:1631–1640. [PubMed: 19103921]
25. Gabbianelli R, Scotti R, Ammendola S, Petrarca P, Nicolini L, Battistoni A. Role of ZnuABC and ZinT in *Escherichia coli* O157:H7 zinc acquisition and interaction with epithelial cells. *BMC Microbiol*. 2011; 11:36. [PubMed: 21338480]
26. Garrido ME, Bosch M, Medina R, Llagostera M, Pérez de Rozas AM, Badiola I, Barbé J. The high-affinity zinc-uptake system *znuACB* is under control of the iron-uptake regulator (*fur*) gene in the animal pathogen *Pasteurella multocida*. *FEMS Microbiol Lett*. 2003; 221:31–37. [PubMed: 12694907]
27. Hood MI, Mortensen BL, Moore JL, Zhang Y, Kehl-Fie TE, Sugitani N, Chazin WJ, Caprioli RM, Skaar EP. Identification of an *Acinetobacter baumannii* zinc acquisition system that facilitates resistance to calprotectin-mediated zinc sequestration. *PLoS Pathog*. 2012; 8:e1003068. [PubMed: 23236280]

28. Karlinsky JE, Maguire ME, Becker LA, Crouch MLV, Fang FC. The phage shock protein PspA facilitates divalent metal transport and is required for virulence of *Salmonella enterica* sv. Typhimurium. *Mol Microbiol.* 2010; 78:669–685. [PubMed: 20807201]
29. Kim S, Watanabe K, Shirahata T, Watarai M. Zinc uptake system (*znuA* locus) of *Brucella abortus* is essential for intracellular survival and virulence in mice. *J Vet Med Sci.* 2004; 66:1059–1063. [PubMed: 15472468]
30. Lewis DA, Klesney-Tait J, Lumbley SR, Ward CK, Latimer JL, Ison CA, Hansen EJ. Identification of the *znuA*-encoded periplasmic zinc transport protein of *Haemophilus ducreyi*. *Infect Immun.* 1999; 67:5060–5068. [PubMed: 10496878]
31. Lim KHL, Jones CE, vanden Hoven RN, Edwards JL, Falsetta ML, Apicella MA, Jennings MP, McEwan AG. Metal binding specificity of the MntABC permease of *Neisseria gonorrhoeae* and its influence on bacterial growth and interaction with cervical epithelial cells. *Infect Immun.* 2008; 76:3569–3576. [PubMed: 18426887]
32. Liu, Janet Z., Jellbauer, S., Poe, AJ., Ton, V., Pesciaroli, M., Kehl-Fie, TE., Restrepo, Nicole A., Hosking, MP., Edwards, Robert A., Battistoni, A., Pasquali, P., Lane, Thomas E., Chazin, Walter J., Vogl, T., Roth, J., Skaar, Eric P., Raffatellu, M. Zinc sequestration by the neutrophil protein calprotectin enhances *Salmonella* growth in the inflamed gut. *Cell Host & Microbe.* 2012; 11:227–239. [PubMed: 22423963]
33. Liu M, Yan M, Liu L, Chen S. Characterization of a novel zinc transporter ZnuA acquired by *Vibrio parahaemolyticus* through horizontal gene transfer. *Front Cell Infect Microbiol.* 2013; 3:61. [PubMed: 24133656]
34. Murphy TF, Brauer AL, Kirkham C, Johnson A, Koszelak-Rosenblum M, Malkowski MG. Role of the zinc uptake ABC transporter of *Moraxella catarrhalis* in persistence in the respiratory tract. *Infect Immun.* 2013; 81:3406–3413. [PubMed: 23817618]
35. Nielubowicz GR, Smith SN, Mobley HLT. Zinc uptake contributes to motility and provides a competitive advantage to *Proteus mirabilis* during experimental urinary tract infection. *Infect Immun.* 2010; 78:2823–2833. [PubMed: 20385754]
36. Plumtre CD, Eijkelkamp BA, Morey JR, Behr F, Couñago RM, Ogunniyi AD, Kobe B, O'Mara ML, Paton JC, McDevitt CA. AdcA and AdcAII employ distinct zinc acquisition mechanisms and contribute additively to zinc homeostasis in *Streptococcus pneumoniae*. *Mol Microbiol.* 2014; 91:834–851. [PubMed: 24428621]
37. Rosadini CV, Gawronski JD, Raimunda D, Argüello JM, Akerley BJ. A novel zinc binding system, ZevAB, is critical for survival of nontypeable *Haemophilus influenzae* in a murine lung infection model. *Infect Immun.* 2011; 79:3366–3376. [PubMed: 21576338]
38. Sabri M, Houle S, Dozois CM. Roles of the extraintestinal pathogenic *Escherichia coli* ZnuACB and ZupT zinc transporters during urinary tract infection. *Infect Immun.* 2009; 77:1155–1164. [PubMed: 19103764]
39. Weston BF, Brenot A, Caparon MG. The metal homeostasis protein, Lsp, of *Streptococcus pyogenes* is necessary for acquisition of zinc and virulence. *Infect Immun.* 2009; 77:2840–2848. [PubMed: 19398546]
40. Yang X, Becker T, Walters N, Pascual DW. Deletion of *znuA* virulence factor attenuates *Brucella abortus* and confers protection against wild-type challenge. *Infect Immun.* 2006; 74:3874–3879. [PubMed: 16790759]
41. Graham AI, Hunt S, Stokes SL, Bramall N, Bunch J, Cox AG, McLeod CW, Poole RK. Severe zinc depletion of *Escherichia coli*: roles for high-affinity zinc binding by ZinT, zinc transport and zinc-independent proteins. *J Biol Chem.* 2009; 284:18377–18389. [PubMed: 19377097]
42. Kehl-Fie TE, Skaar EP. Nutritional immunity beyond iron: a role for manganese and zinc. *Curr Opin Chem Biol.* 2010; 14:218–224. [PubMed: 20015678]
43. Petrarca P, Ammendola S, Pasquali P, Battistoni A. The Zur-regulated ZinT protein is an auxiliary component of the high-affinity ZnuABC zinc transporter that facilitates metal recruitment during severe zinc shortage. *J Bacteriol.* 2010; 192:1553–1564. [PubMed: 20097857]
44. Grass G, Wong MD, Rosen BP, Smith RL, Rensing C. ZupT Is a Zn(II) uptake system in *Escherichia coli*. *J Bacteriol.* 2002; 184:864–866. [PubMed: 11790762]

45. Bobrov AG, Kirillina O, Fetherston JD, Miller MC, Burlison JA, Perry RD. The *Yersinia pestis* siderophore, yersiniabactin, and the ZnuABC system both contribute to Zinc acquisition and the development of lethal septicemic plague in mice. *Mol Microbiol.* 2014; 93:759–775. [PubMed: 24979062]
46. Citiulo F, Jacobsen ID, Miramón P, Schild L, Brunke S, Zipfel P, Brock M, Hube B, Wilson D. *Candida albicans* scavenges host zinc via Pra1 during endothelial invasion. *PLoS Pathog.* 2012; 8:e1002777. [PubMed: 22761575]
47. Cortese MS, Paszczynski A, Lewis TA, Sebat JL, Borek V, Crawford RL. Metal chelating properties of pyridine-2,6-bis(thiocarboxylic acid) produced by *Pseudomonas* spp. and the biological activities of the formed complexes. *BioMetals.* 2002; 15:103–120. [PubMed: 12046919]
48. Leach LH, Morris JC, Lewis TA. The role of the siderophore pyridine-2,6-bis (thiocarboxylic acid) (PDTC) in zinc utilization by *Pseudomonas putida* DSM 3601. *BioMetals.* 2007; 20:717–726. [PubMed: 17066327]
49. Hesketh A, Kock H, Mootien S, Bibb M. The role of *absC*, a novel regulatory gene for secondary metabolism, in zinc-dependent antibiotic production in *Streptomyces coelicolor* A3(2). *Mol Microbiol.* 2009; 74:1427–1444. [PubMed: 19906184]
50. Zhao B, Moody SC, Hider RC, Lei L, Kelly SL, Waterman MR, Lamb DC. Structural analysis of cytochrome P450 105N1 involved in the biosynthesis of the zincophore, coelibactin. *Int J Mol Sci.* 2012; 13:8500–8513. [PubMed: 22942716]
51. Braud A, Geoffroy V, Hoegy F, Mislin GLA, Schalk IJ. Presence of the siderophores pyoverdine and pyochelin in the extracellular medium reduces toxic metal accumulation in *Pseudomonas aeruginosa* and increases bacterial metal tolerance. *Environ Microbiol Rpt.* 2010; 2:419–425.
52. Braud A, Hannauer M, Mislin GLA, Schalk IJ. The *Pseudomonas aeruginosa* pyochelin-iron uptake pathway and its metal specificity. *J Bacteriol.* 2009; 191:3517–3525. [PubMed: 19329644]
53. Braud A, Hoegy F, Jezequel K, Lebeau T, Schalk IJ. New insights into the metal specificity of the *Pseudomonas aeruginosa* pyoverdine - iron uptake pathway. *Environ Microbiol.* 2009; 11:1079–1091. [PubMed: 19207567]
54. Nakai H, Kobayashi S, Ozaki M, Hayase Y, Takeda R. Micacocidin A. *Acta Crystallogr.* 1999; C55:54–56.
55. Kreutzer MF, Kage H, Gebhardt P, Wackler B, Saluz HP, Hoffmeister D, Nett M. Biosynthesis of a complex yersiniabactin-like natural product via the *mic* Locus in phytopathogen *Ralstonia solanacearum*. *Appl Environ Microbiol.* 2011; 77:6117–6124. [PubMed: 21724891]
56. Gong S, Bearden SW, Geoffroy VA, Fetherston JD, Perry RD. Characterization of the *Yersinia pestis* Yfu ABC iron transport system. *Infect Immun.* 2001; 67:2829–2837.
57. Fetherston JD, Kirillina O, Bobrov AG, Paulley JT, Perry RD. The yersiniabactin transport system is critical for the pathogenesis of bubonic and pneumonic plague. *Infect Immun.* 2010; 78:2045–2052. [PubMed: 20160020]
58. Staggs TM, Perry RD. Identification and cloning of a *fur* regulatory gene in *Yersinia pestis*. *J Bacteriol.* 1991; 173:417–425. [PubMed: 1898928]
59. Desrosiers DC, Bearden SW, Mier I Jr, Abney J, Paulley JT, Fetherston JD, Salazar JC, Radolf JD, Perry RD. Znu is the predominant zinc importer in *Yersinia pestis* during *in vitro* growth but is not essential for virulence. *Infect Immun.* 2010; 78:5163–5177. [PubMed: 20855510]
60. Price PA, Jin J, Goldman WE. Pulmonary infection by *Yersinia pestis* rapidly establishes a permissive environment for microbial proliferation. *Proc Natl Acad Sci USA.* 2012; 109:3083–3088. [PubMed: 22308352]
61. Dunn SD. Effects of the modification of transfer buffer composition and the renaturation of proteins in gels on the recognition of proteins on western blots by monoclonal antibodies. *Anal Biochem.* 1986; 157:144–153. [PubMed: 3532863]
62. Miller MC, DeMoll E. Extraction, purification, and Identification of yersiniabactin, the siderophore of *Yersinia pestis*. *Curr Prot Microbiol.* 2011; 23:5B.3.1–5B.3.22.
63. Miller MC, Fetherston JD, Pickett CL, Bobrov AG, Weaver RH, DeMoll E, Perry RD. Reduced synthesis of the Ybt siderophore or production of aberrant Ybt-like molecules activates transcription of yersiniabactin genes in *Yersinia pestis*. *Microbiology.* 2010; 156:2226–2238. [PubMed: 20413552]

64. Drechsel H, Stephan H, Lotz R, Haag H, Zähner H, Hantke K, Jung G. Structure elucidation of yersiniabactin, a siderophore from highly virulent *Yersinia* strains. *Liebigs Ann.* 1995; 1995:1727–1733.
65. Hunt JB, Neece SH, Ginsburg A. The use of 4-(2-pyridylazo)resorcinol in studies of zinc release from *Escherichia coli* aspartate transcarbamoylase. *Anal Biochem.* 1985; 146:150–157. [PubMed: 3887984]
66. Liu Y, Kochi A, Pithadia AS, Lee S, Nam Y, Beck MW, He X, Lee D, Lim MH. Tuning reactivity of diphenylpropynone derivatives with metal-associated amyloid- $\beta$  species via structural modifications. *Inorg Chem.* 2013; 52:8121–8130. [PubMed: 23805940]
67. Fosso MY, LeVine H 3rd, Green KD, Tsodikov OV, Garneau-Tsodikova S. Effects of structural modifications on the metal binding, anti-amyloid activity, and cholinesterase inhibitory activity of chalcones. *Org Biomol Chem.* 2015; 13:9418–9426. [PubMed: 26248214]
68. Reed LJ, Muench H. A simple method for estimating fifty percent endpoints. *Am J Hyg.* 1938; 27:493–497.
69. Ray A, Dittel BN. Isolation of mouse peritoneal cavity cells. *J Vis Exp.* 2010; 35:1488.
70. Sun Y, Connor MG, Pennington JM, Lawrenz MB. Development of bioluminescent bioreporters for *in vitro* and *in vivo* tracking of *Yersinia pestis*. *PLoS ONE.* 2012; 7:e47123. [PubMed: 23071730]
71. Fetherston JD, Bertolino VJ, Perry RD. YbtP and YbtQ: two ABC transporters required for iron uptake in *Yersinia pestis*. *Mol Microbiol.* 1999; 32:289–299. [PubMed: 10231486]
72. Pechous RD, Broberg CA, Stasulli NM, Miller VL, Goldman WE. *In vivo* transcriptional profiling of *Yersinia pestis* reveals a novel bacterial mediator of pulmonary inflammation. *mBio.* 2015; 6
73. Neyrolles O, Wolschendorf F, Mitra A, Niederweis M. Mycobacteria, metals, and the macrophage. *Immunol Rev.* 2015; 264:249–263. [PubMed: 25703564]
74. Botella H, Stadthagen G, Lugo-Villarino G, de Chastellier C, Neyrolles O. Metallobiology of host-pathogen interactions: an intoxicating new insight. *Trends Microbiol.* 2012; 20:106–112. [PubMed: 22305804]
75. Djoko KY, Ong CIY, Walker MJ, McEwan AG. The role of copper and zinc toxicity in innate immune defense against bacterial pathogens. *J Biol Chem.* 2015; 290:18954–18961. [PubMed: 26055706]
76. Abergel RJ, Clifton MC, Pizarro JC, Warner JA, Shuh DK, Strong RK, Raymond KN. The siderocalin/enterobactin interaction: a link between mammalian immunity and bacterial iron transport. *J Am Chem Soc.* 2008; 130:11524–11534. [PubMed: 18680288]
77. German N, Doyscher D, Rensing C. Bacterial killing in macrophages and amoeba: do they all use a brass dagger? *Future Microbiol.* 2013; 8:1257–1264. [PubMed: 24059917]
78. Navarrete F, De La Fuente L. Zinc detoxification is required for full virulence and modification of the host leaf ionome by *Xylella fastidiosa*. *Mol Plant Microbe Interact.* 2015; 28:497–507. [PubMed: 25561271]
79. Botella H, Peyron P, Levillain F, Poincloux R, Poquet Y, Brandli I, Wang C, Tailleur L, Tilleul S, Charrière GM, Waddell SJ, Foti M, Lugo-Villarino G, Gao Q, Maridonneau-Parini I, Butcher PD, Castagnoli PR, Gicquel B, de Chastellier C, Neyrolles O. Mycobacterial P<sub>1</sub>-type ATPases mediate resistance to zinc poisoning in human macrophages. *Cell Host Microbe.* 2011; 10:248–259. [PubMed: 21925112]
80. Stähler FN, Odenbreit S, Haas R, Wilrich J, Van Vliet AH, Kusters JG, Kist M, Bereswill S. The novel *Helicobacter pylori* CznABC metal efflux pump is required for cadmium, zinc, and nickel resistance, urease modulation, and gastric colonization. *Infect Immun.* 2006; 74:3845–3852. [PubMed: 16790756]
81. Goguen JD, Yother J, Straley SC. Genetic analysis of the low calcium response in *Yersinia pestis* Mu d1 (*Ap lac*) insertion mutants. *J Bacteriol.* 1984; 160:842–848. [PubMed: 6094509]
82. Pujol C, Bliska JB. The ability to replicate in macrophages is conserved between *Yersinia pestis* and *Yersinia pseudotuberculosis*. *Infect Immun.* 2003; 71:5892–5899. [PubMed: 14500510]
83. Pujol C, Klein KA, Romanov GA, Palmer LE, Ciota C, Zhao Z, Bliska JB. *Yersinia pestis* can reside in autophagosomes and avoid xenophagy in murine macrophages by preventing vacuole acidification. *Infect Immun.* 2009; 77:2251–2261. [PubMed: 19289509]

84. Connor MG, Pulsifer AR, Price CT, Abu Kwaik Y, Lawrenz MB. *Yersinia pestis* requires host Rab1b for survival in macrophages. *PLoS Pathog.* 2015; 11:e1005241. [PubMed: 26495854]
85. Spinner JL, Winfree S, Starr T, Shannon JG, Nair V, Steele-Mortimer O, Hinnebusch BJ. *Yersinia pestis* survival and replication within human neutrophil phagosomes and uptake of infected neutrophils by macrophages. *J Leukoc Biol.* 2014; 95:389–398. [PubMed: 24227798]
86. Rensing C, Mitra B, Rosen BP. The *zntA* gene of *Escherichia coli* encodes a Zn(II)-translocating P-type ATPase. *PNAS.* 1997; 94:14326–14331. [PubMed: 9405611]
87. Sebbane F, Lemaître N, Sturdevant DE, Rebeil R, Virtaneva K, Porcella SF, Hinnebusch BJ. Adaptive response of *Yersinia pestis* to extracellular effectors of innate immunity during bubonic plague. *Proc Natl Acad Sci U S A.* 2006; 103:11766–11771. [PubMed: 16864791]
88. Vadyvaloo V, Jarrett C, Sturdevant DE, Sebbane F, Hinnebusch BJ. Transit through the flea vector induces a pretransmission innate immunity resistance phenotype in *Yersinia pestis*. *PLoS Pathog.* 2010; 6:e1000783. [PubMed: 20195507]
89. Fillat MF. The FUR (ferric uptake regulator) superfamily: Diversity and versatility of key transcriptional regulators. *Arch Biochem Biophys.* 2014; 546:41–52. [PubMed: 24513162]
90. Li Y, Qiu Y, Gao H, Guo Z, Han Y, Song Y, Du Z, Wang X, Zhou D, Yang R. Characterization of Zur-dependent genes and direct Zur targets in *Yersinia pestis*. *BMC Microbiol.* 2009; 9:128. [PubMed: 19552825]
91. Geoffroy VA, Fetherston JD, Perry RD. *Yersinia pestis* YbtU and YbtT are involved in synthesis of the siderophore yersiniabactin but have different effects on regulation. *Infect Immun.* 2000; 68:4452–4461. [PubMed: 10899842]
92. Perry RD, Abney J, Mier I Jr, Lee Y, Bearden SW, Fetherston JD. Regulation of the *Yersinia pestis* Yfe and Ybt iron transport systems. *Adv Exp Med Biol.* 2003; 529:275–283. [PubMed: 12756771]
93. Chaturvedi KS, Hung CS, Crowley JR, Stapleton AE, Henderson JP. The siderophore yersiniabactin binds copper to protect pathogens during infection. *Nat Chem Biol.* 2012; 8:731–736. [PubMed: 22772152]
94. Koh EI, Hung CS, Parker KS, Crowley JR, Giblin DE, Henderson JP. Metal selectivity by the virulence-associated yersiniabactin metallophore system. *Metallomics.* 2015; 7:1011–1022. [PubMed: 25824627]
95. Youard Z, Wenner N, Reimann C. Iron acquisition with the natural siderophore enantiomers pyochelin and enantio-pyochelin in *Pseudomonas* species. *BioMetals.* 2011; 24:513–522. [PubMed: 21188474]
96. Choi JS, Braymer JJ, Nanga RPR, Ramamoorthy A, Lim MH. Design of small molecules that target metal-A $\beta$  species and regulate metal-induced A $\beta$  aggregation and neurotoxicity. *Proc Natl Acad Sci USA.* 2010; 107:21990–21995. [PubMed: 21131570]
97. Porcheron G, Garénaux A, Proulx J, Sabri M, Dozois CM. Iron, copper, zinc, and manganese transport and regulation in pathogenic Enterobacteria: correlations between strains, site of infection and the relative importance of the different metal transport systems for virulence. *Front Cell Infect Microbiol.* 2013; 3:90. [PubMed: 24367764]
98. Perry RD, Bobrov AG, Fetherston JD. The role of transition metal transporters for iron, zinc, manganese, and copper in the pathogenesis of *Yersinia pestis*. *Metallomics.* 2015; 7:965–978. [PubMed: 25891079]
99. Perry RD, Bobrov AG, Kirillina O, Rhodes ER, Actis LA, Fetherston JD. *Yersinia pestis* transition metal divalent cation transporters. *Adv Exp Med Biol.* 2012; 954:267–279. [PubMed: 22782773]
100. Fetherston JD, Mier I Jr, Truszczynska H, Perry RD. The Yfe and Feo transporters are involved in microaerobic growth and the virulence of *Yersinia pestis* in bubonic plague. *Infect Immun.* 2012; 80:3880–3891. [PubMed: 22927049]
101. Perry RD, Craig SK, Abney J, Bobrov AG, Kirillina O, Mier I Jr, Truszczynska H, Fetherston JD. Manganese transporters Yfe and MntH are Fur-regulated and important for the virulence of *Yersinia pestis* in bubonic plague. *Microbiology.* 2012; 158:804–815. [PubMed: 22222497]
102. Brickman T, Armstrong S. Temporal signaling and differential expression of *Bordetella* iron transport systems: the role of ferrimones and positive regulators. *BioMetals.* 2009; 22:33–41. [PubMed: 19130264]

103. Lathem WW, Crosby SD, Miller VL, Goldman WE. Progression of primary pneumonic plague: a mouse model of infection, pathology, and bacterial transcriptional activity. *Proc Natl Acad Sci U S A*. 2005; 102:17786–17791. [PubMed: 16306265]
104. Fetherston JD, Lillard JW Jr, Perry RD. Analysis of the pesticin receptor from *Yersinia pestis*: role in iron-deficient growth and possible regulation by its siderophore. *J Bacteriol*. 1995; 177:1824–1833. [PubMed: 7896707]
105. Kem MP, Zane HK, Springer SD, Gauglitz JM, Butler A. Amphiphilic siderophore production by oil-associating microbes. *Metallomics*. 2014; 6:1150–1155. [PubMed: 24663669]
106. Zane HK, Naka H, Rosconi F, Sandy M, Haygood MG, Butler A. Biosynthesis of amphiphilic siderophores by *Vibrio harveyi* BAA-1116: identification of a bifunctional nonribosomal peptide synthetase condensation domain. *J Am Chem Soc*. 2014; 136:5615–5618. [PubMed: 24701966]
107. Martinez JS, Butler A. Marine amphiphilic siderophores: marinobactin structure, uptake, and microbial partitioning. *J Inorg Biochem*. 2007; 101:1692–1698. [PubMed: 17868890]
108. Gauglitz JM, Iinishi A, Ito Y, Butler A. Microbial tailoring of acyl peptidic siderophores. *Biochemistry*. 2014; 53:2624–2631. [PubMed: 24735218]
109. Kage H, Kreutzer MF, Wackler B, Hoffmeister D, Nett M. An iterative type I polyketide synthase initiates the biosynthesis of the antimycoplasmal agent micacocidin. *Chem Biol*. 2013; 20:764–771. [PubMed: 23790487]
110. Kobayashi S, Nakai H, Ikenishi Y, Sun WY, Ozaki M, Hayase Y, Takeda R. Micacocidin A, B and C, novel antimycoplasmal agents from *Pseudomonas* sp. II. Structure elucidation. *J Antibiot (Tokyo)*. 1998; 51:328–332. [PubMed: 9589069]
111. Wang T, Si M, Song Y, Zhu W, Gao F, Wang Y, Zhang L, Zhang W, Wei G, Luo ZQ, Shen X. Type VI secretion system transports Zn<sup>2+</sup> to combat multiple stresses and host immunity. *PLoS Pathog*. 2015; 11:e1005020. [PubMed: 26134274]
112. Ghssein G, Brutesco C, Ouerdane L, Fojcik C, Izaute A, Wang S, Hajjar C, Lobinski R, Lemaire D, Richaud P, Voulhoux R, Espaillat A, Cava F, Pignol D, Borezée-Durant E, Arnoux P. Biosynthesis of a broad-spectrum nicotianamine-like metallophore in *Staphylococcus aureus*. *Science*. 2016; 352:1105–1109. [PubMed: 27230378]
113. Remy L, Carrière M, Derré-Bobillot A, Martini C, Sanguinetti M, Borezée-Durant E. The *Staphylococcus aureus* Opp1 ABC transporter imports nickel and cobalt in zinc-depleted conditions and contributes to virulence. *Mol Microbiol*. 2013; 87:730–743. [PubMed: 23279021]
114. Forman S, Paulley JT, Fetherston JD, Cheng YQ, Perry RD. *Yersinia* ironomics: comparison of iron transporters among *Yersinia pestis* biotypes and its nearest neighbor, *Yersinia pseudotuberculosis*. *BioMetals*. 2010; 23:275–294. [PubMed: 20049509]



### Significance to Metallomics

This study shows that the ability to acquire zinc during infection is critical for *Yersinia pestis* to cause bubonic and pneumonic plague. Two different zinc transporters are important for growth in mice. While one system compensates for the loss of the other, loss of both causes a drastic loss of virulence. One system involves the yersiniabactin (Ybt) siderophore (important for iron uptake). While the Ybt siderophore does not directly bind zinc, our results suggest that Ybt plus a second molecule or a modified Ybt participates in or promotes Zn-binding and is involved in the ability of *Y. pestis* to obtain zinc.

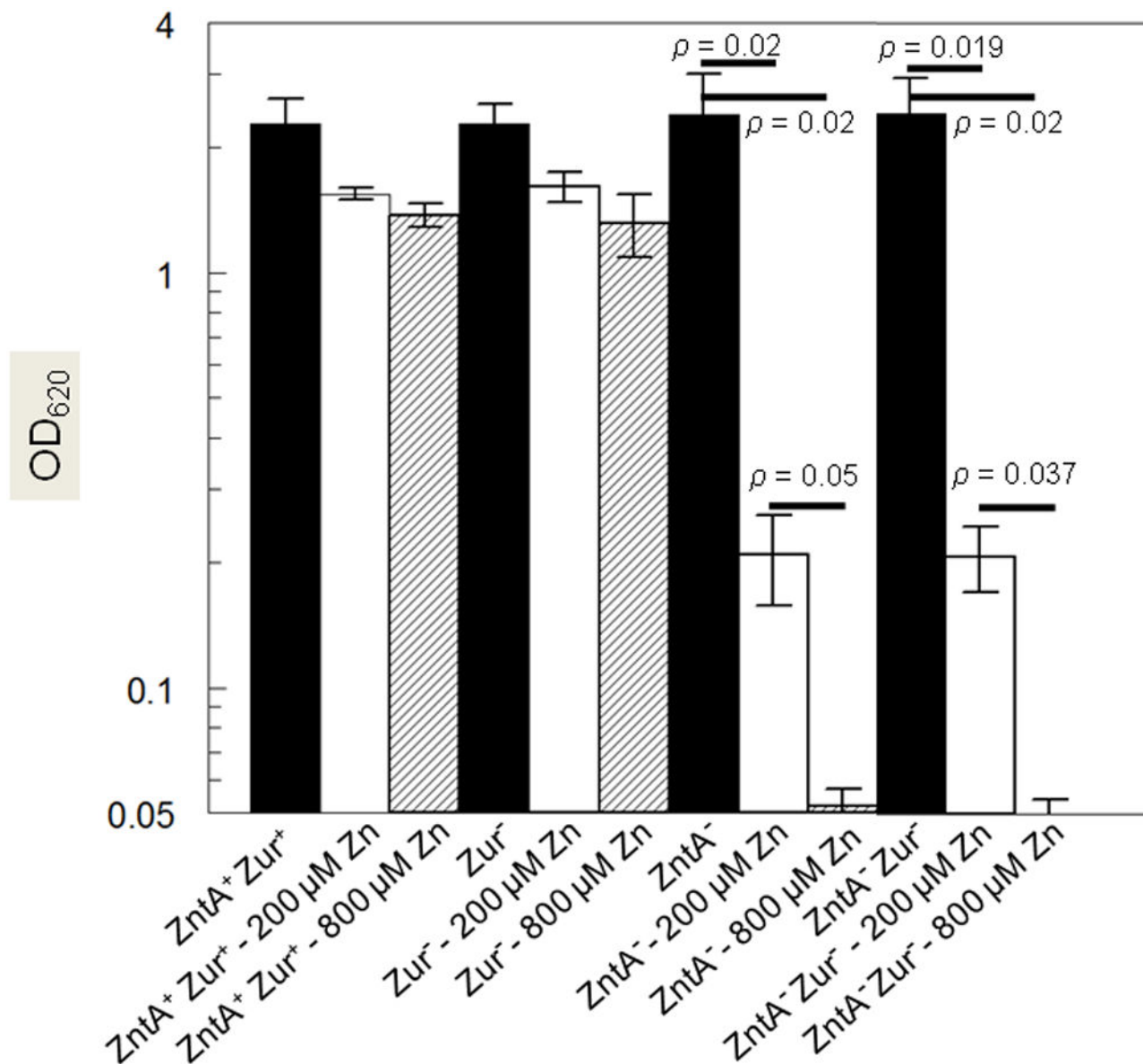


**Fig. 1. ZntA but not Zur is required for *Y. pestis* growth under high Zn<sup>2+</sup> conditions**

Growth rates of *Y. pestis* KIM6+ (ZntA<sup>+</sup> Zur<sup>+</sup> parental strain), KIM6-2078+ (Zur<sup>-</sup>; *zur::kan*), KIM6-2196.1+ (ZntA<sup>-</sup>; *zntA*) and KIM6-2196.4+ (ZntA<sup>-</sup> Zur<sup>-</sup>; *zntA zur::kan*) in HIB-FS without or with supplementation to 200 and 800 μM ZnCl<sub>2</sub>. Numbers are averages from three independent experiments or cultures. Standard deviations and statistical significances are shown.

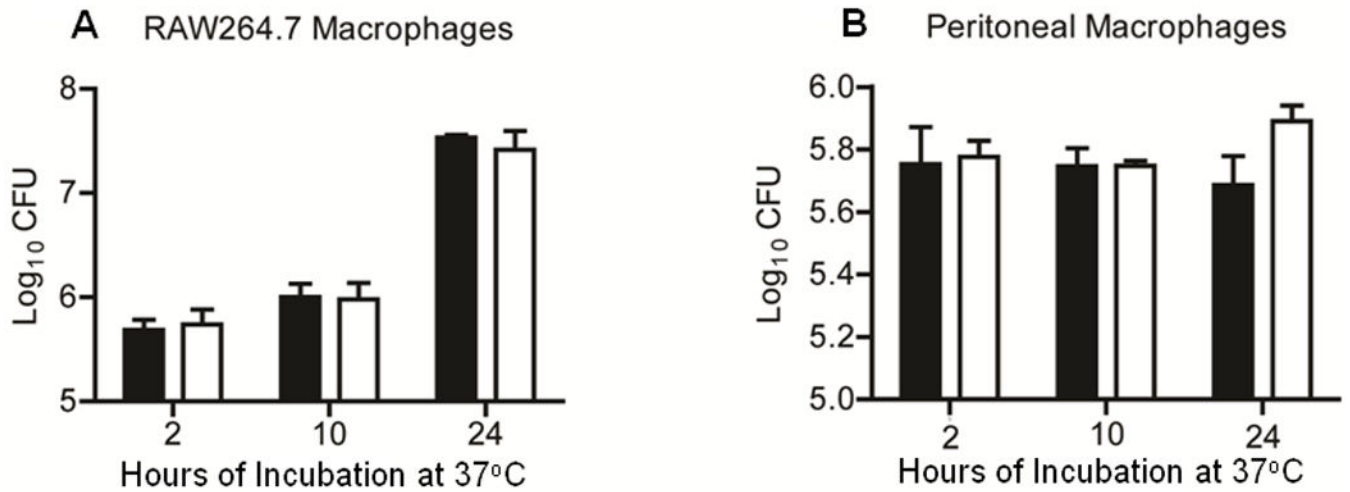


**Fig. 2. The *zntA zur::kan* mutant is not attenuated for survival in macrophages**  
 $1.0 \times 10^5$  (A) RAW274.6 (n=3 samples/time point) or (B) peritoneal macrophages (n=3 samples/time point) were infected with *Y. pestis* KIM6+ (*ZntA*<sup>+</sup> *Zur*<sup>+</sup>) or KIM6-2196.4+ (*ZntA*<sup>-</sup> *Zur*<sup>-</sup>; *zntA zur::kan*) at an MOI of 10. Extracellular bacteria were killed with gentamicin and intracellular bacteria were quantified at 2, 10, and 24 h post-infection. Patterns for RAW274.6 cells (growth) and peritoneal macrophages (survival but not growth) are typical for *Y. pestis*.

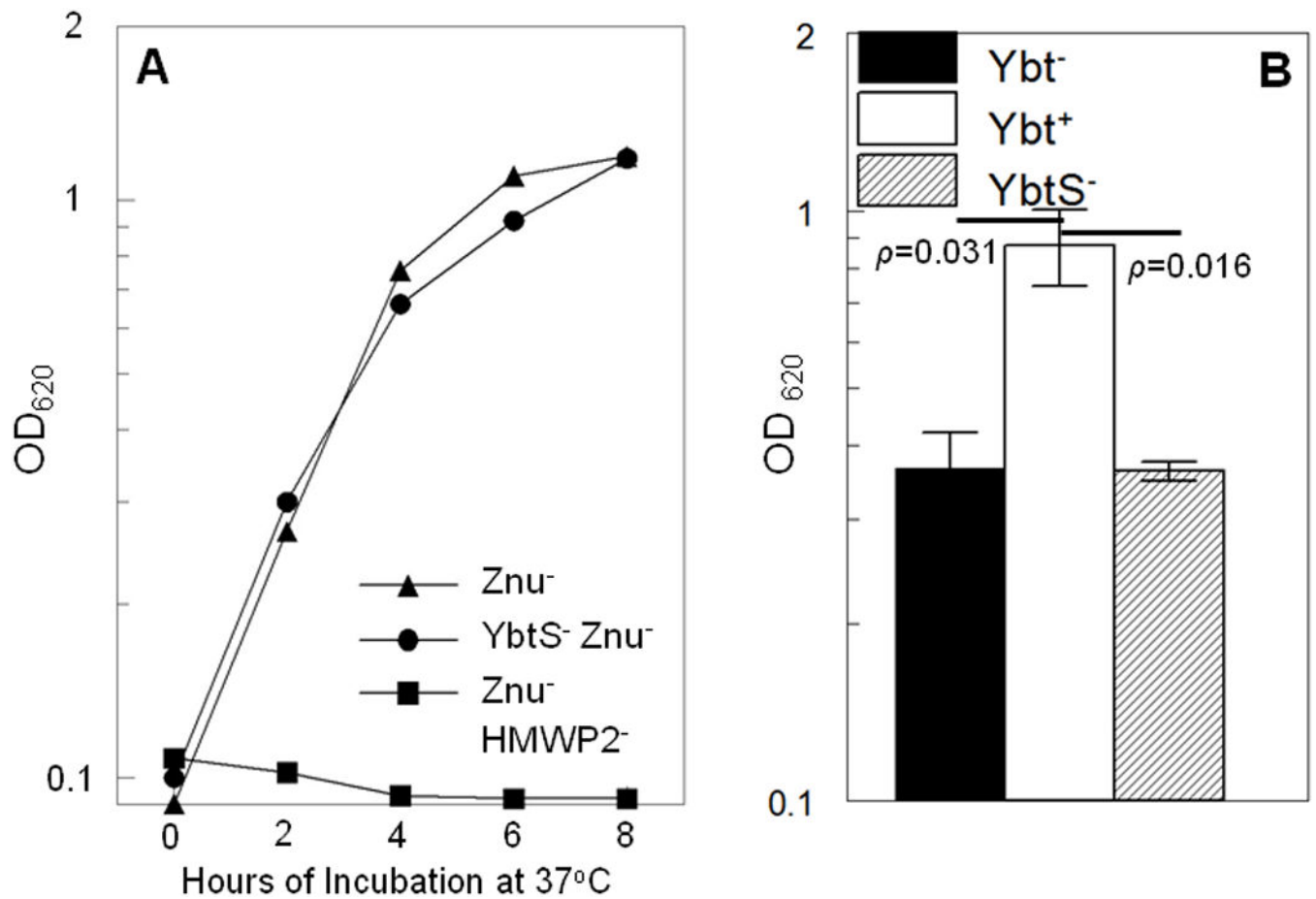


**Fig. 3. YbtS is not required for growth of the *znu* mutant under low  $Zn^{2+}$  conditions**

Panel A. Growth rates of *Y. pestis* KIM6-2077+ ( $Znu^{-}$ ; *znuBC*), KIM6-2070.3 ( $YbtS^{-}$   $Znu^{-}$ ; *ybtS::kan znuBC*) and KIM6-2077.7 ( $HMWP2^{-}$   $Znu^{-}$ ; *irp2::kan znuBC*) in cPMH2 supplemented with 0.6  $\mu M$   $ZnCl_2$  and 1  $\mu M$   $FeCl_3$ . Panel B. After acclimation to growth at 37°C in cPMH2 supplemented with 0.6  $\mu M$   $ZnCl_2$  and 1.0  $\mu M$   $FeCl_3$ , cultures of KIM6-2077.18 ( $HMWP2^{-}$   $Psn^{-}$   $Znu^{-}$ ; *irp2::kan psn znuBC*) were back diluted to an  $OD_{620}$  of  $\sim 0.1$  in a 1:1 mixture of the same medium with filtered culture supernatants from KIM6-2046.1 ( $Ybt^{-}$ ; *irp2::kan*), KIM6+ ( $Ybt^{+}$  parent strain) and KIM6-2070.1 ( $YbtS^{-}$ ; *ybtS::kan*). Numbers are averages from multiple samples from at least two independent experiments. Standard deviations and statistical significances are shown.

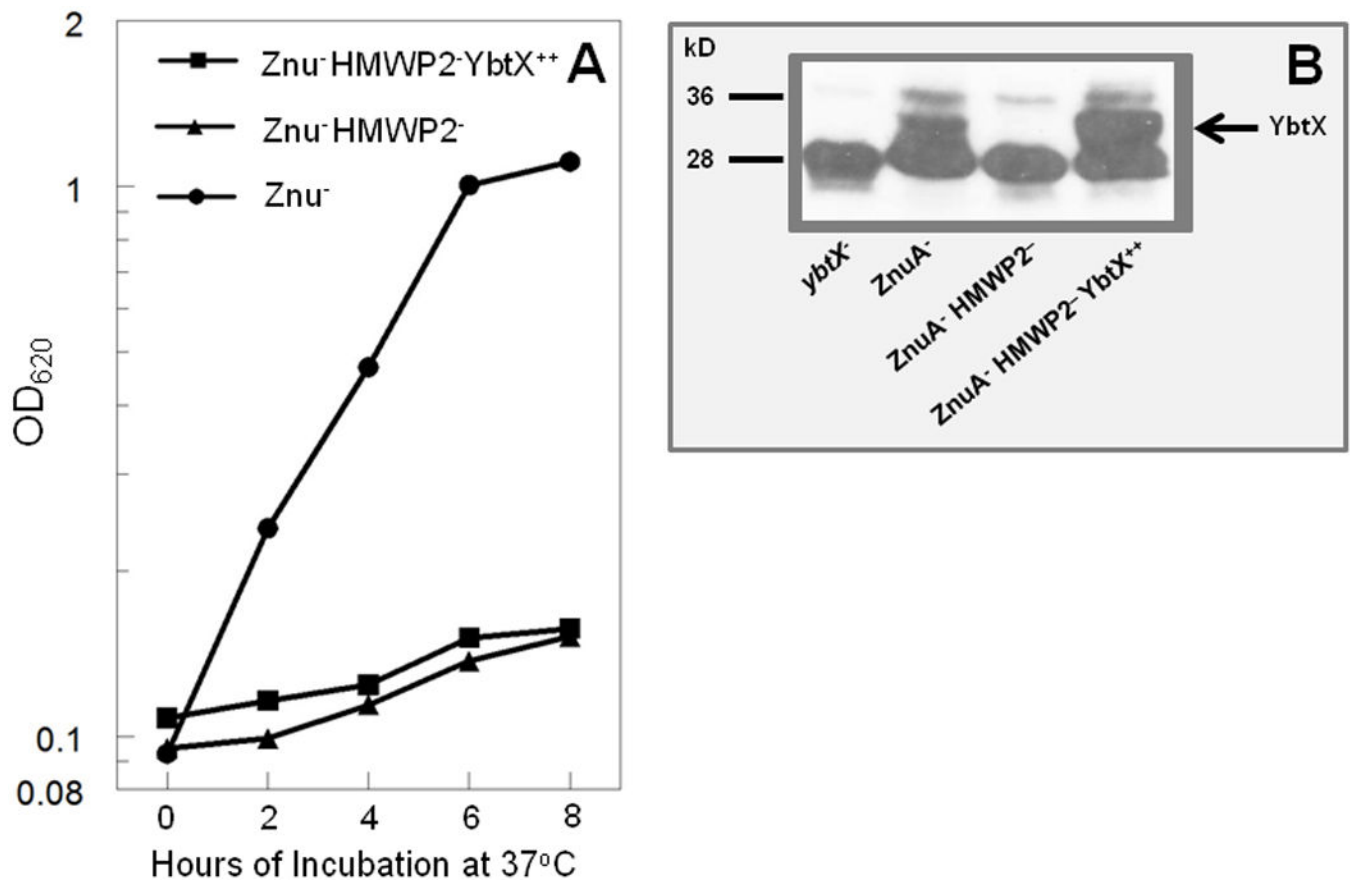


**Fig. 4. Overexpression of YbtX does not restore the growth defect of double *Znu*<sup>-</sup> HMWP2<sup>-</sup> mutants under low Zn conditions**

Panel A: Growth of *Y. pestis* KIM6-2197(pACYC184)<sup>+</sup> (*Znu*<sup>-</sup>; *znuA*) and KIM6-2197.1 carrying pACYC184 (*Znu*<sup>-</sup> HMWP2<sup>-</sup>; *irp2 znuA*) or pYbtX-ZP (*Znu*<sup>-</sup> HMWP2<sup>-</sup> YbtX<sup>++</sup>; *irp2 znuA ybtX<sup>++</sup>*) in cPMH2 supplemented with 0.6 μM ZnCl<sub>2</sub> and 1 μM FeCl<sub>3</sub>. Overexpression of *ybtX<sup>++</sup>* is driven by the *znuA* promoter. Panel B: Analysis of YbtX expression by Western blot with antiserum against YbtX. KIM6-2067 (*YbtX*<sup>-</sup>; *ybtS::kan*) is a negative control. The growth curves and Western blot shown are representative of results from two or more independent experiments.

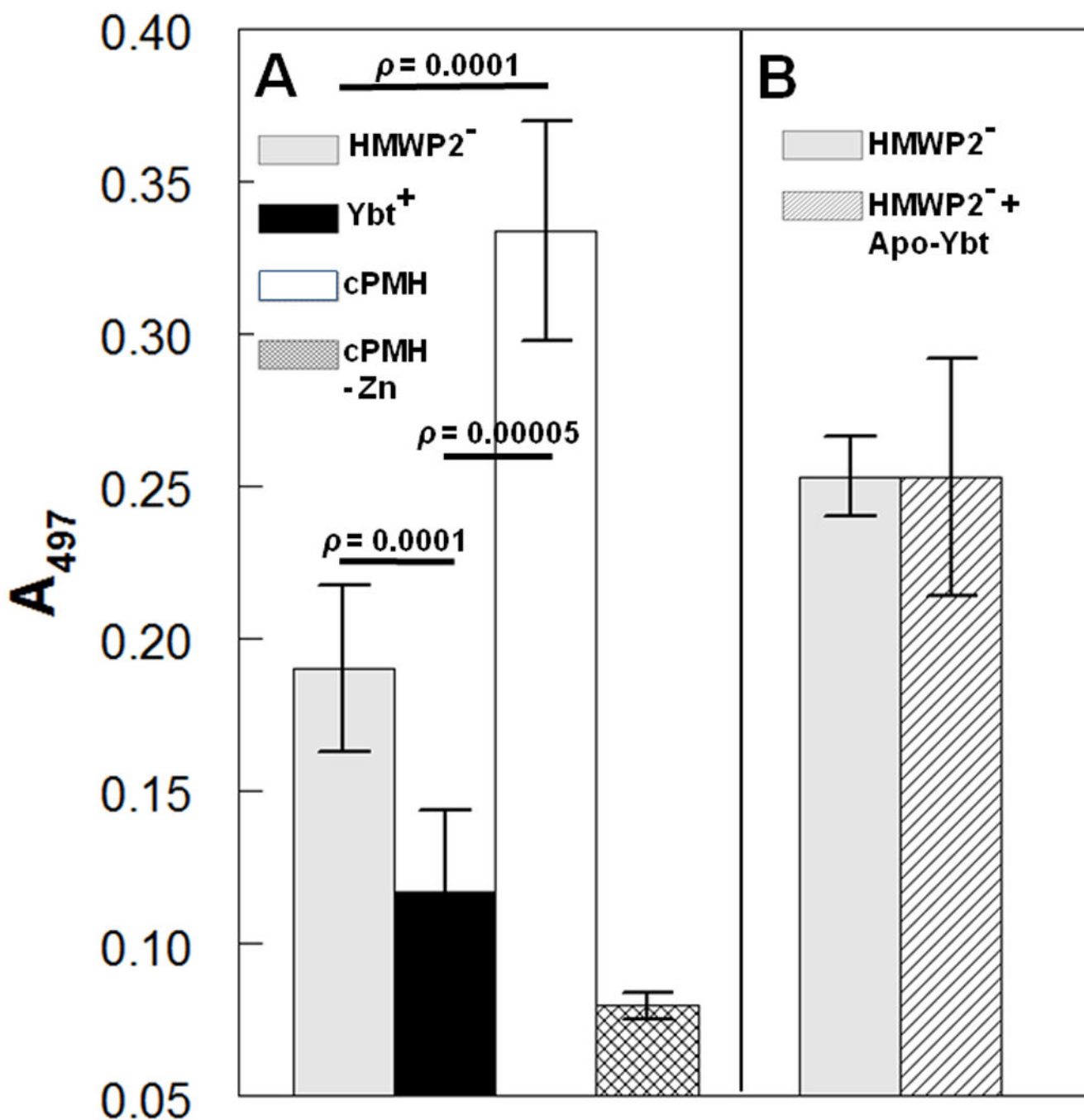


**Fig. 5. PAR assay for detection of Zn<sup>2+</sup>-binding activity in culture supernatants**

Filtered supernatants of Ybt producing (KIM6+; Ybt<sup>+</sup>) and a non-producing strain (KIM6-2046.1; HMWP2<sup>-</sup>; *irp2::kan*) (A) grown in cPMH medium for 30 hours at 37°C were incubated with 3 μM (A - supernatant samples) or 5 μM (B - purified apo-Ybt) ZnCl<sub>2</sub> in a PAR reaction buffer before PAR was added to 50 μM. cPMH with or without 3 μM ZnCl<sub>2</sub> was used as a control. When the PAR assay is performed without added Zn<sup>2+</sup>, the absorbance change due to Zn<sup>2+</sup> binding is further reduced as expected. In panel B, apo-Ybt was added to the KIM6-2046.1 supernatant to directly test Zn<sup>2+</sup> binding by apo-Ybt. Results

are the average from at least 6 (A) or 2-4 (B) independent samples. Statistical significances are indicated.

Author Manuscript

Author Manuscript

Author Manuscript

Author Manuscript

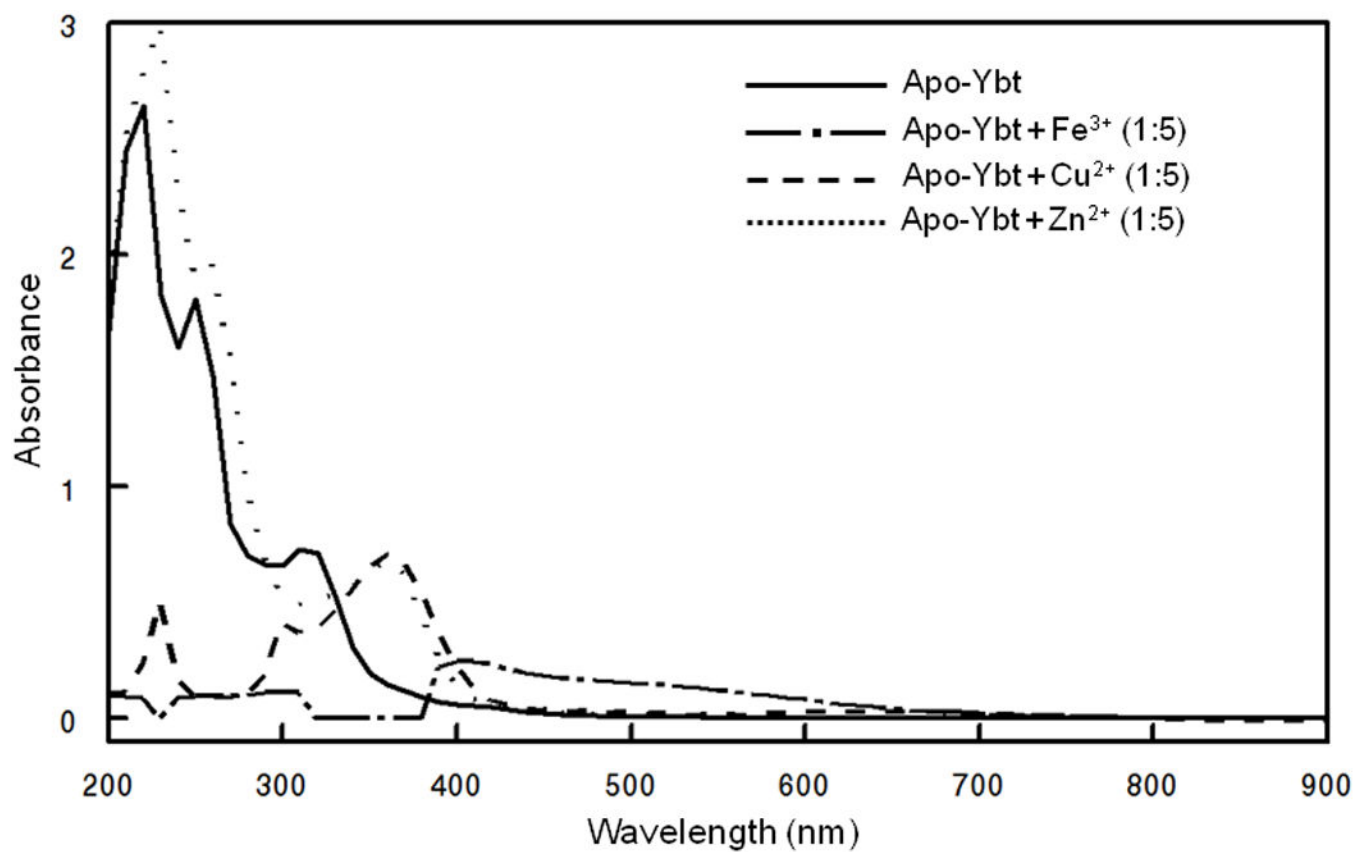


**Fig. 6. UV-Vis absorption spectra of apo-Ybt and Ybt + Fe<sup>3+</sup>, Cu<sup>2+</sup>, or Zn<sup>2+</sup>**  
Metals were added to apo-Ybt at a concentration 5-fold higher than the apo-Ybt concentration two minutes prior to spectroscopic measurements from 200-900 nm.



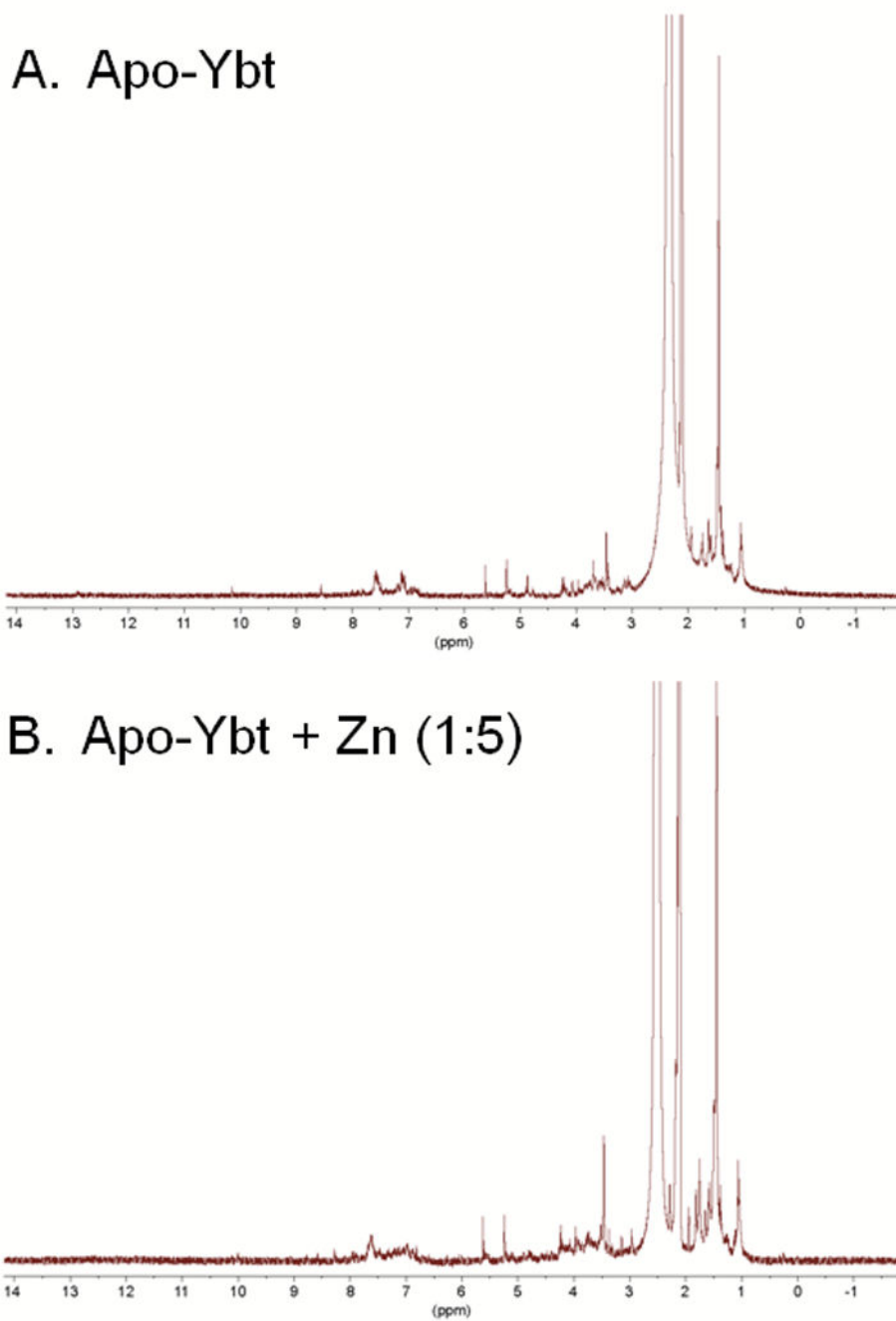
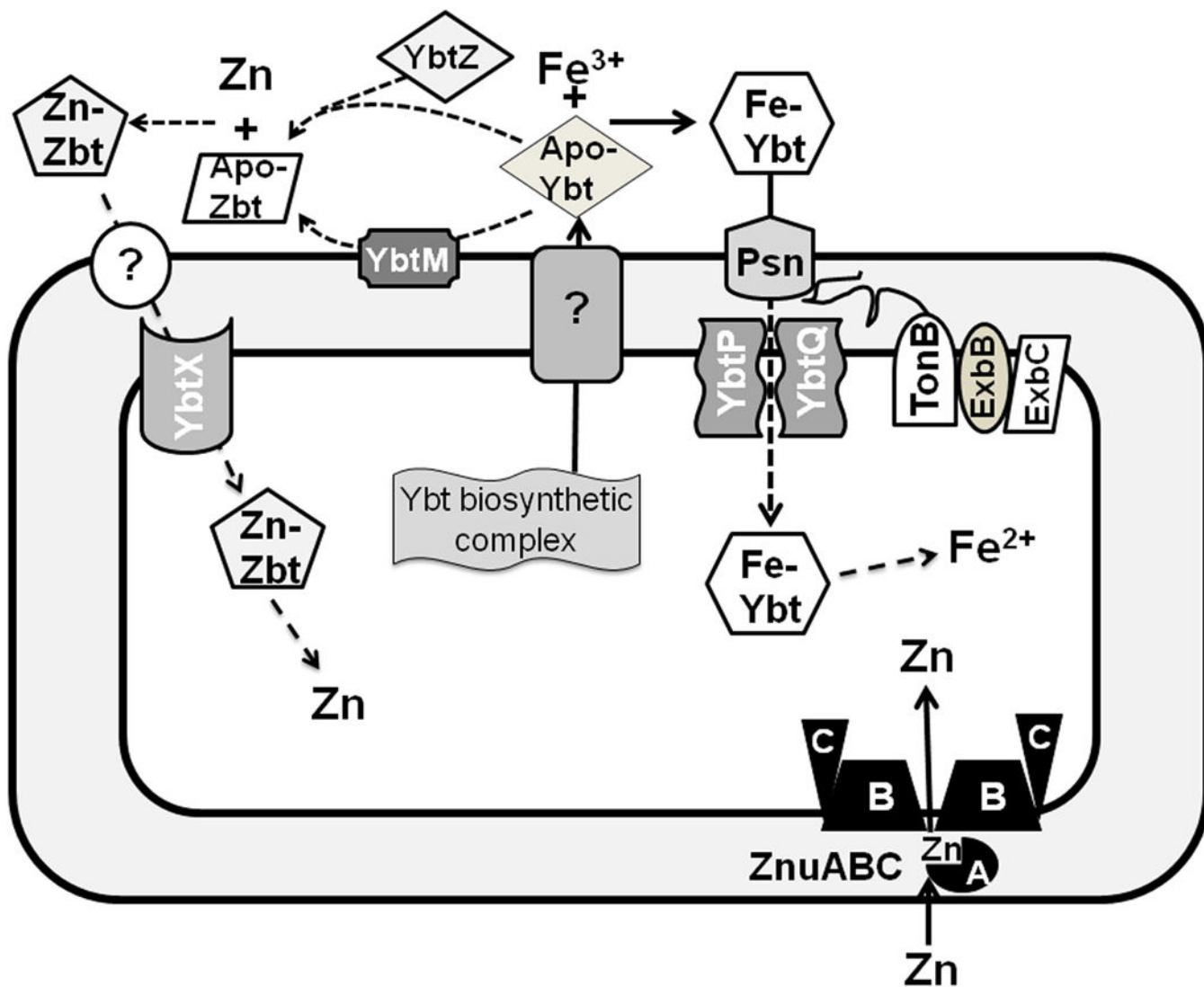


Fig. 7. <sup>1</sup>H NMR spectra of apo-Ybt and apo-Ybt + Zn<sup>2+</sup> (1:5)



**Fig. 8. Model of proposed  $Zn^{2+}$  transport in *Y. pestis***

The ZnuABC transporter is typical of other Gram-negative ZnuABC systems. For the Ybt systems, the mechanisms for export of apo-Ybt and removal of Fe from the siderophore have not been established. In addition, entry of the Fe-Ybt chelate into the cell has not been demonstrated (dashed arrows indicate tentative pathways). Use of Fe from Ybt does require the TonB-dependent OM receptor, Psn and the YbtPQ ABC IM transporter (solid arrows indicate proven pathways). Current evidence supports two models for the role of Ybt in  $Zn^{2+}$  uptake. A putative surface exposed enzyme (YbtM) modifies Ybt such that it binds  $Zn^{2+}$ . Alternatively, exported apo-ybt may interact with another putative exported compound (YbtZ) to generate a Ybt-YbtZ  $Zn^{2+}$  binding complex (tentatively termed apo-Zbt for both models). In the second model, YbtZ is degraded in the absence of apo-Ybt. If an OM receptor or porin is required for  $Zn^{2+}$  uptake via YbtX, it is not TonB dependent. As for Fe-Ybt, there is no evidence for or against entry of the  $Zn^{2+}$ -Zbt complex into the cell.

**Table 1**  
**Virulence of *Y. pestis* strains in mouse models of bubonic, pneumonic and septicemic plague**

| Strain or mutation <sup>a</sup> | Pneumonic plague LD <sub>50</sub> <sup>b</sup>                                | Bubonic plague LD <sub>50</sub> <sup>b</sup>                                  | Septicemic plague LD <sub>50</sub> <sup>b</sup> |
|---------------------------------|---|---|---|
| Parent strain                   | 129 [329 ± 105]   | <14 [25 ± 12]   | <14 ± 1.4                                       |
| <i>znuA</i>                     | 715 ± 619   | 52 ± 58   | ~11 ± 5   |
| <i>ybtX</i>                     | 434 ± 231   | 176 ± 171 <sup>c</sup>  | Not tested                                      |
| <i>ybtX znuA</i>                | >1.6 × 10 <sup>6</sup> ± 2.2 × 10 <sup>5</sup> (>1.2 × 10 <sup>4</sup> -fold) | >8.9 × 10 <sup>6</sup> ± 1.6 × 10 <sup>5</sup> (>6.4 × 10 <sup>5</sup> -fold) | Not tested                                      |
| <i>ybtX<sup>DP</sup> znu</i>    | 976 ± 66  | 32 ± 33 (NS)  | Not tested                                      |
| <i>ybtS::kan znuBC</i>          | Not tested  | Not tested  | 5.3 × 10 <sup>6</sup> ± 1.2 10 <sup>4</sup>     |
| <i>zntA zur::kan</i>            | 1,237 ± 656   | 17.8 ± 0.4  | Not tested                                      |

<sup>a</sup>Strains: parent - KIM5(pCD1Ap)<sup>+</sup> (Ybt<sup>+</sup> Znu<sup>+</sup>); *znuA* - KIM5-2197(pCD1Ap)<sup>+</sup>; *ybtX* - KIM5-2067(pCD1Ap); *ybtX znuA* - KIM5-2197.2(pCD1Ap); *ybtX<sup>DP</sup> znu* - KIM5-2197.4(pCD1Ap)<sup>+</sup> [ *ybtX* mutation replaced with *ybtX<sup>T</sup>*]; *ybtS::kan znuBC* - KIM5-2070.3(pCD1Ap); *zntA zur::kan* - KIM5-2196.4(pCD1Ap)<sup>+</sup>

<sup>b</sup>Standard deviations are shown with the fold virulence losses (compared to the parent strain) shown in parentheses, where relevant. Results for the parent strain are from one trial in the pneumonic and bubonic plague models used as a positive control; previous results from multiple trials with the same parent strain<sup>57</sup> are shown in brackets.

<sup>c</sup>One of three trials had a calculated LD<sub>50</sub> of <13 (lowest dose).